

Accepted Manuscript

Design, synthesis and activity of Mnk1 and Mnk2 selective inhibitors containing thieno[2,3-*d*]pyrimidine scaffold

Xin Jin, James Merrett, Sheng Tong, Bartholomew Flower, Jianling Xie, Rilei Yu, Shuye Tian, Ling Gao, Jiajun Zhao, Xuemin Wang, Tao Jiang, Christopher G. Proud



PII: S0223-5234(18)30947-4

DOI: <https://doi.org/10.1016/j.ejmech.2018.10.070>

Reference: EJMECH 10856

To appear in: *European Journal of Medicinal Chemistry*

Received Date: 22 May 2018

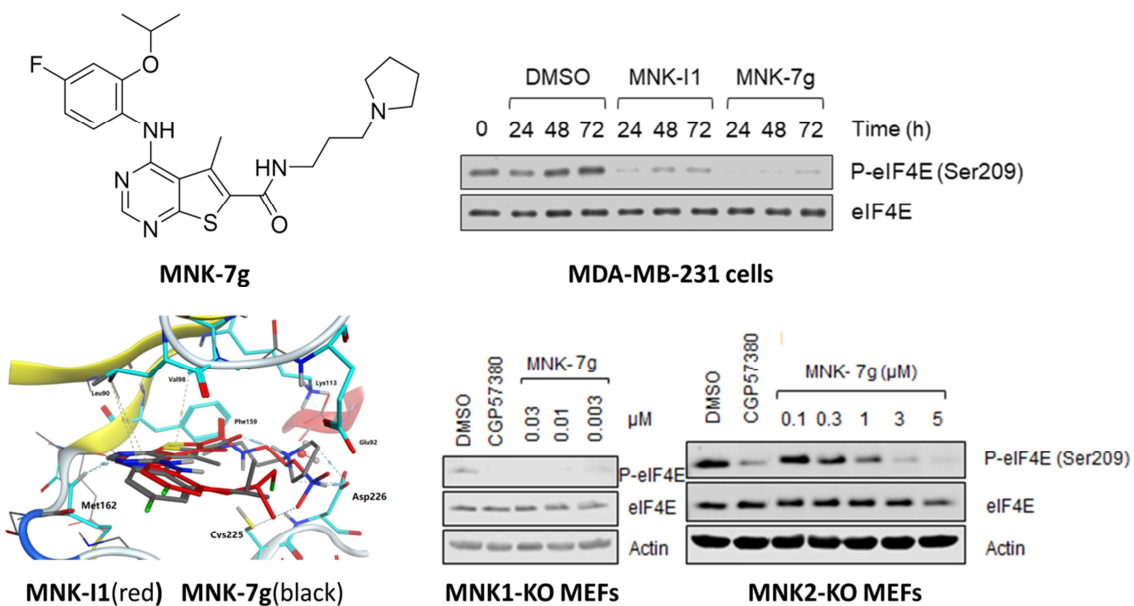
Revised Date: 25 October 2018

Accepted Date: 31 October 2018

Please cite this article as: X. Jin, J. Merrett, S. Tong, B. Flower, J. Xie, R. Yu, S. Tian, L. Gao, J. Zhao, X. Wang, T. Jiang, C.G. Proud, Design, synthesis and activity of Mnk1 and Mnk2 selective inhibitors containing thieno[2,3-*d*]pyrimidine scaffold, *European Journal of Medicinal Chemistry* (2018), doi: <https://doi.org/10.1016/j.ejmech.2018.10.070>.

This is a PDF file of an unedited manuscript that has been accepted for publication. As a service to our customers we are providing this early version of the manuscript. The manuscript will undergo copyediting, typesetting, and review of the resulting proof before it is published in its final form. Please note that during the production process errors may be discovered which could affect the content, and all legal disclaimers that apply to the journal pertain.

Graphical Abstracts



ACCEPTED TEL

Design, synthesis and activity of Mnk1 and Mnk2 selective inhibitors containing thieno[2,3-d]pyrimidine scaffold

¹[#]Xin Jin, ²[#]James Merrett, ¹Sheng Tong, ²Bartholomew Flower, ²Jianling Xie, ¹Rilei Yu, ²Shuye Tian, ⁴Ling Gao, ⁴Jiajun Zhao, ^{2,3}Xuemin Wang, ¹Tao Jiang* and ^{2,3}Christopher G. Proud*

¹School of Medicine and Pharmacy, Ocean University of China, and Laboratory for Marine Drugs and Bioproducts, Qingdao National Laboratory for Marine Science and Technology, Qingdao, China; ²Nutrition & Metabolism, South Australian Health & Medical Research Institute, North Terrace, Adelaide, SA5000, Australia; ³School of Biological Sciences, University of Adelaide, Adelaide SA5005, Australia, ⁴Department of Endocrinology, Shandong Provincial Hospital Affiliated to Shandong University, Shandong, China.

[#] *These authors contributed equally to this study.*

ABSTRACT

The mitogen-activated protein kinase-interacting kinases 1 and 2 (MNK1 and MNK2) phosphorylate eukaryotic initiation factor 4E (eIF4E) and play important roles in promoting tumorigenesis and metabolic disease. Thus, inhibiting these enzymes might be valuable in the treatment of such conditions. We designed and synthesized a series of 4-((4-fluoro-2-isopropoxyphenyl)amino)-5-methylthieno[2,3-d]pyrimidine derivatives, and evaluated their inhibitory activity against the MNKs. We found 15 compounds that were active as MNK inhibitors and that one in particular, designated **MNK-7g**, which was potent against MNK1 and substantially more potent against MNK2. The compound **MNK-7g** did not affect other signaling pathways tested and had no adverse effects on cell viability. As expected from earlier studies, **MNK-7g** also inhibited cell migration. Therefore, the compound **MNK-7g**, which forms an ionic bond with Asp226 in MNK2 and possesses a substituted aniline in a thieno[2,3-d] pyrimidine structure, is a promising starting point for the future development of novel drugs for treating or managing cancer and metabolic disease.

KEYWORDS : Mnk; eIF4E Inhibition; Thieno[2,3-d]pyrimidine; Selective inhibitor

1. INTRODUCTION:

The MAP kinase-interacting kinases (also termed MAP kinase signal-integrating kinases, MNKs) are activated by phosphorylation of their activation loops by certain members of the MAP kinase (MAPK) superfamily [1-5]. The different isoforms of MNKs (MNK1 and MNK2) each phosphorylate the translation initiation factor eIF4E [3-5]. eIF4E binds to the 5'-cap structure which is found on all cytoplasmic mRNAs in eukaryotes. It also interacts with other initiation factors and thereby plays a crucial role in recruiting ribosomes to mRNAs, thereby promoting the initiation of their translation [6].

eIF4E is implicated in tumorigenesis and cancer progression (for a review, see [7, 8]), and several lines of data suggest that phosphorylation of eIF4E is important in solid tumors and in specific settings in leukemia (see, for example, [9-11] and discussion in [7]). MNKs also promote the migration of cancer cells and may therefore play a role in tumor metastasis [12-14]. It remains unclear how eIF4E phosphorylation promotes tumor formation and progression, although a number of mechanisms have been proposed [7]. eIF4E phosphorylation and/or the MNKs also play roles in other processes such as innate immunity and macrophage activation [15, 16].

We recently showed that mice lacking MNK1 or MNK2 are protected against the adverse effects of a high-fat diet [17]. For example, they show lower weight gain, improved glucose tolerance and better sensitivity to insulin than high fat-fed wild-type mice. Interestingly, MNK1-KO and MNK2-KO mice are protected in distinct ways; on a high fat diet, MNK2-KO mice show lower weight gain and much less adipose tissue inflammation than wild-type animals, while MNK1-KO mice show similar levels of these parameters to high fat-fed wild-type mice, but still show

improved insulin signaling and glucose tolerance [17]. Thus, MNKs may be valid targets for the management of metabolic disorders associated with excessive caloric intake and obesity. Inhibiting the MNKs has therapeutic potential for cancers or metabolic syndrome, especially since MNKs are not essential in normal cells or indeed in mice under standard vivarium conditions [18]. Specific inhibitors of the MNKs are therefore expected to show low, if any, toxicity.

Although several compounds that inhibit MNKs have been reported, agents such as cercosporamide or CGP57380 [19] (Fig. 1) exert off-target effects on other kinases, inhibiting several of them with greater potency than the MNKs [20]. This made it important to identify novel selective MNK inhibitors. Recently, two MNK inhibitors have entered the clinical research stage, in different settings, BAY1143269 (chemical structure not published) [21] and eFT508 [22] (Fig. 1). Meanwhile, merestinib (Fig. 1), which is in clinical testing in an ongoing phase 1 study, was reported as an orally bioavailable small-molecule multi-kinase inhibitor exerting good inhibitory effect on the MNKs [23]. This compound has been studied in acute myeloid leukemia (AML) [23]. In addition, a new inhibitor, SEL-201 (Fig. 1 [13]), was found to exert potent anti-melanoma effects by blocking MNK1/2 [13]. Lastly, a further MNK inhibitor was reported; it is being evaluated for the treatment of blast crisis leukemia [24].

Some recent patent applications have revealed the structures of thienopyrimidine compounds with low nanomolar efficacy in inhibiting the MNKs. However, detailed selectivity and efficacy data have not yet been presented. Previously, we reported a novel compound, MNK-I1 [12] (Fig. 1) as a more potent and specific inhibitor of the MNKs than either CGP57380 or cercosporamide. In cells, it inhibits the activities of MNK1 and MNK2 at low micromolar concentrations [12]. While it is the best MNK inhibitor that is readily available, it has poor

stability and requires a complicated synthetic process, making it less than ideal. Studies from Wang's group have revealed some new chemical skeletons of MNK inhibitors [25-28] and indicate that substitution at the *ortho*-position of the fluoroaniline ring of this structure and substituent at the C6-position of thienopyrimidine may significantly enhance the potency and selectivity of these compounds [25].

In developing further potential inhibitors, we had three aims: (i) to obtain compounds with enhanced potency against the MNKs; (ii) to identify compounds with selectivity for MNK2 over MNK1 and (iii) to simplify the synthetic route. As initial steps in that direction, we set out to determine which modifications to MNK-I1 were compatible with retention of inhibitory activity against MNKs and, through computer modeling, gain insights into the structure-activity relationship (SAR) of these compounds as inhibitors of MNK2. Here, we describe the synthesis and biological evaluation of the new compounds.

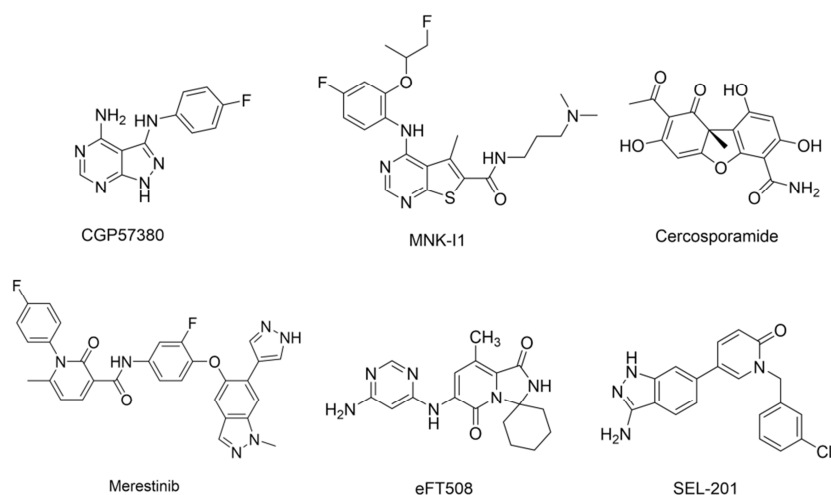


Figure 1. Structures of recently-reported MNK inhibitors.

2. RESULTS & DISCUSSION:

2.1 Identifying active analogs of MNK-II: initial set of compounds

MNK1 and MNK2 share ~80% sequence identity within their catalytic domains [3]. Based on their sequences, the MNKs belong to the Ca^{2+} /calmodulin-dependent kinase group, but are not regulated by Ca^{2+} /calmodulin. Instead, the MNKs are activated by MAPK signaling pathways [29]. Although targeting the MNKs holds the potential for treating cancer [7], little success has been achieved in this area so far, partly due to the lack of small molecule inhibitors for them which are sufficiently potent or specific and are also suitable for use *in vivo*. The protein databank (PDB) contains crystal structures for MNK1 (PDB ID: 2hw6) and MNK2 (PDB ID: 2ac3, PDB ID: 2hw7), albeit in inactive states where key residues in their activation loops are not phosphorylated and their conformations are consequently not those of the active enzymes. The MNK proteins possess a unique Asp-Phe-Asp (DFD) motif, which replaces the Asp-Phe-Gly (DFG) motif found in all other protein kinases [30, 31]. Moreover, this DFD motif adopts an unusual 'DFD-out' conformation, in which the Phe residue flips into the ATP binding pocket, thereby blocking access for ATP and exposing an additional hydrophobic/allosteric site [32]. In the crystal structure of MNK2 (PDB ID: 2hw7) the kinase inhibitor staurosporine binds in the ATP-binding site promoting the kinase-active conformation to move toward the 'DFG/D in' configuration.

Due to the unique DFD motif, the MNKs possess a small hydrophobic pocket near the gatekeeper which is formed by the Phe159 gatekeeper and Cys225 secondary gatekeeper residues. The MNKs also have a larger cavity near the lower hinge region than many kinases; this lies in a C-shaped loop owing to a hydrogen bond between Met162 and Gly165 [33]. These

features could in principle be exploited to develop specific MNK inhibitors. We used the docking software, MOE, to examine the binding mode of staurosporine to MNK2. The interaction map between staurosporine and MNK2 provides important information about their interactions: two hydrogen bonds with Glu160 and Met162 from the hinge region and the third one with Glu92 (Fig. 2A). MNK-I1 inhibits MNKs potently with good selectivity, i.e., with little effect on other protein kinases, and blocks the migration of cancer cells [12]. We docked compound MNK-I1 into the binding site of MNK2, as shown in Fig. 2B, to assess its mode of interaction at this binding site. Molecular docking revealed several key interactions, including two hydrogen bonds involving (i) the N atom of the pyrimidine and (ii) the N atom of the C6-position amide bond of MNK-I1 with Met162 from the hinge region, and one ionic bond between the alkaline group at the C6-position of the thienopyrimidine of MNK-I1 and Asp226 from DFD motif. Fig. 2B indicated that the fluorine atom at the *ortho*-position of fluoroaniline did not interact with any residues from the surface of MNK2. Since the fluorine at this position complicates the synthesis, we decided to alter it, while keeping other groups the same.

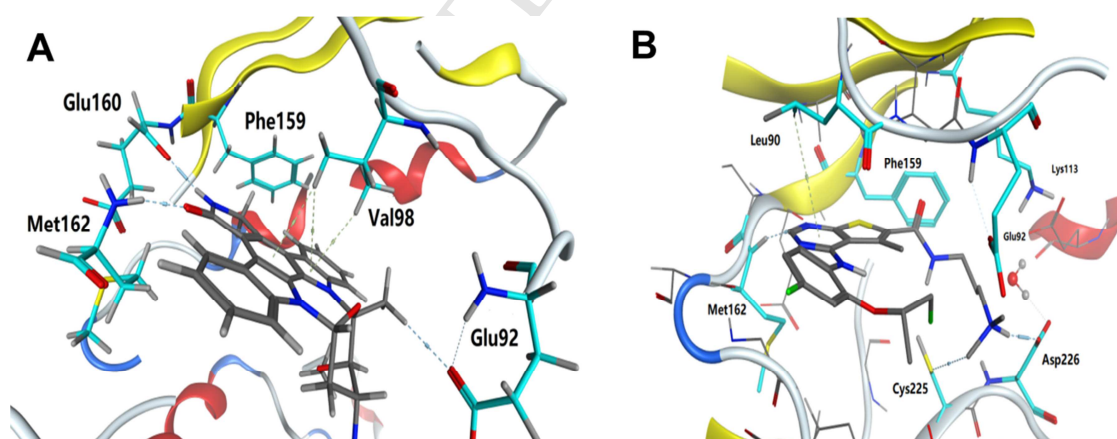


Figure 2. View of inhibitors (staurosporine and MNK-I1) in the pocket of MNK2. **(A)** Stereoview of staurosporine in ATP binding site of MNK2, showing the required key interactions with MNK2. **(B)** The binding mode of MNK-I1 in the pocket of MNK2. Compound stick representation: carbon in black, nitrogen in blue, oxygen in red, sulfur in yellow, and fluorine in green. Light blue shows the amino acid residues in MNK2.

With this result in mind, at the first stage of the compound design process, we synthesized five compounds according to reference [25]. They included **7w** with an isopropyl ether group, and **7v** with methoxyl group instead of the fluorinated isopropyl ether group, respectively; two compounds **7x** and **6d** derived from **7w** and one further compound **3b** (see Fig. 3 and Scheme 1). The activity of these compounds against MNKs was tested by treating mouse 3T3-L1 cells to assess the level of phosphorylation of eIF4E. eIF4E is the best-characterized and only *in vivo*-validated substrate for the MNKs [17]. It is phosphorylated by MNK1 or MNK2, but by no other kinases, as shown by the complete loss of eIF4E phosphorylation in cells and tissues from mice in which the genes for MNK1 and MNK2 (*Mknk1* and *Mknk2*) have been disrupted [18]. MNKs phosphorylate eIF4E exclusively on Ser209 [34]. Thus, phosphorylation of eIF4E provides a reliable and diagnostic ‘read-out’ of MNK activity within cells.

Apart from MNK-I1, the compounds were inactive (**7v**, **3b**) or only weakly active (**6d**, **7x**) against MNKs in 3T3-L1 cells (data were summarized in Fig. 3). **7w** was the most effective, but was less potent than MNK-I1 (did not inhibit P-eIF4E completely, unlike MNK-I1). Although we did not obtain better compounds than MNK-I1, this indicated that altering the fluorinated isopropyl ether group in the compound (MNK-I1) allowed activity to be retained. We also suspected that the substituent group at the C6-position of thienopyrimidine itself had a

substantial influence on the ability of the compound to inhibit the MNKs when other substituents were kept the same.

We therefore focused on the C6-position. At the second stage of the compound design process, we changed the substituent at C6-position of the thienopyrimidine to obtain a series of compounds, **7f**, **7g**, **7a** and **6c** as shown in Fig. 3. We chose some polar and bulkier groups and changed the lengths of the carbon chains of the substituent (**7a-u** in Scheme 2). We also used an ester bond instead of an amide bond in the substituent (**6a-c** in Scheme 2).

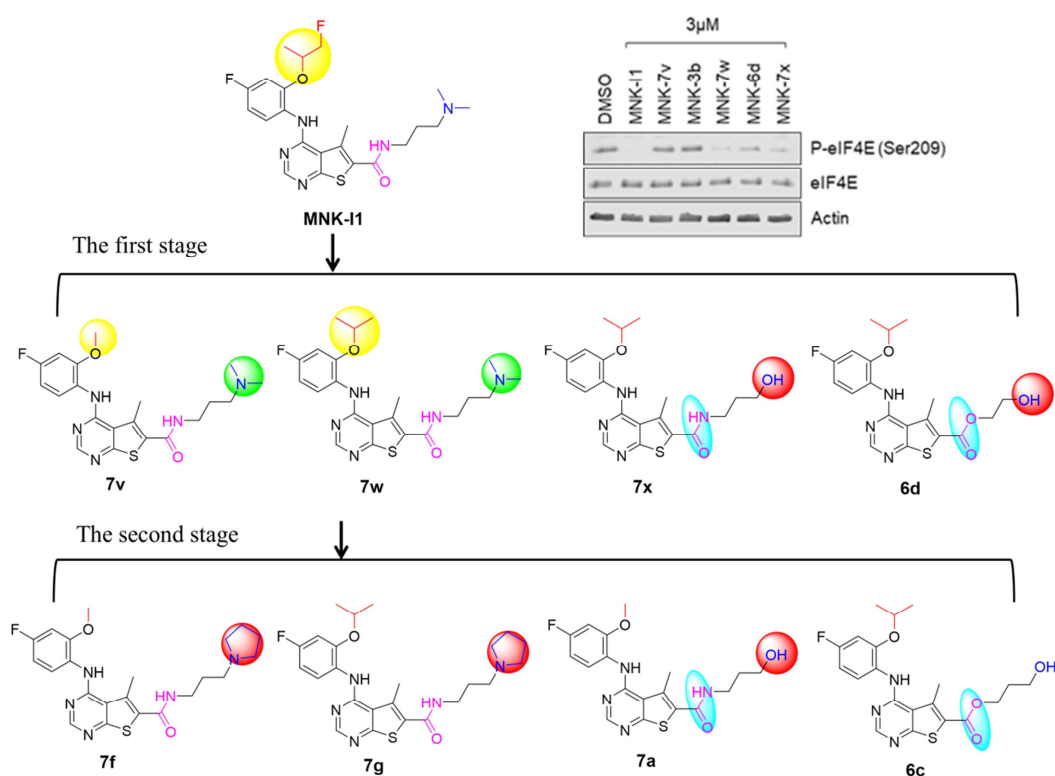
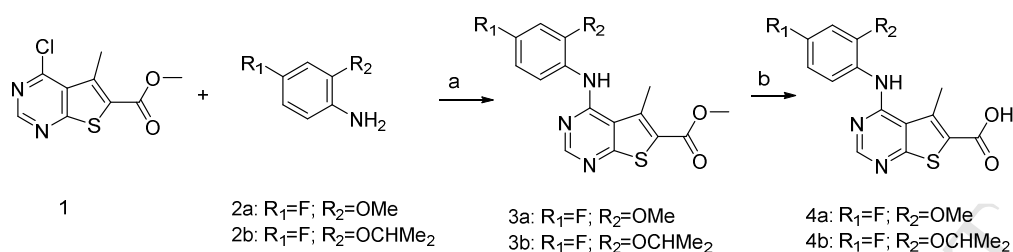


Figure 3. Structural modification of MNK-I1 and the activity against MNKs of the compounds (**3b**, **6d**, **7v**, **7w** and **7x**). In the first stage, we modified the *ortho*-position of the substituted aniline (**7v**, **7w**) and the C6-position (**7x**, **6d**). Subsequently, based on the first stage, we focused on the C6-position to obtain a series of derivatives. Their activity was tested in 3T3-L1 cells

which were treated with the indicated compounds for 2 h. Cells were then lysed, and lysate supernatants analysed by SDS-PAGE and western blot using the indicated antibodies.

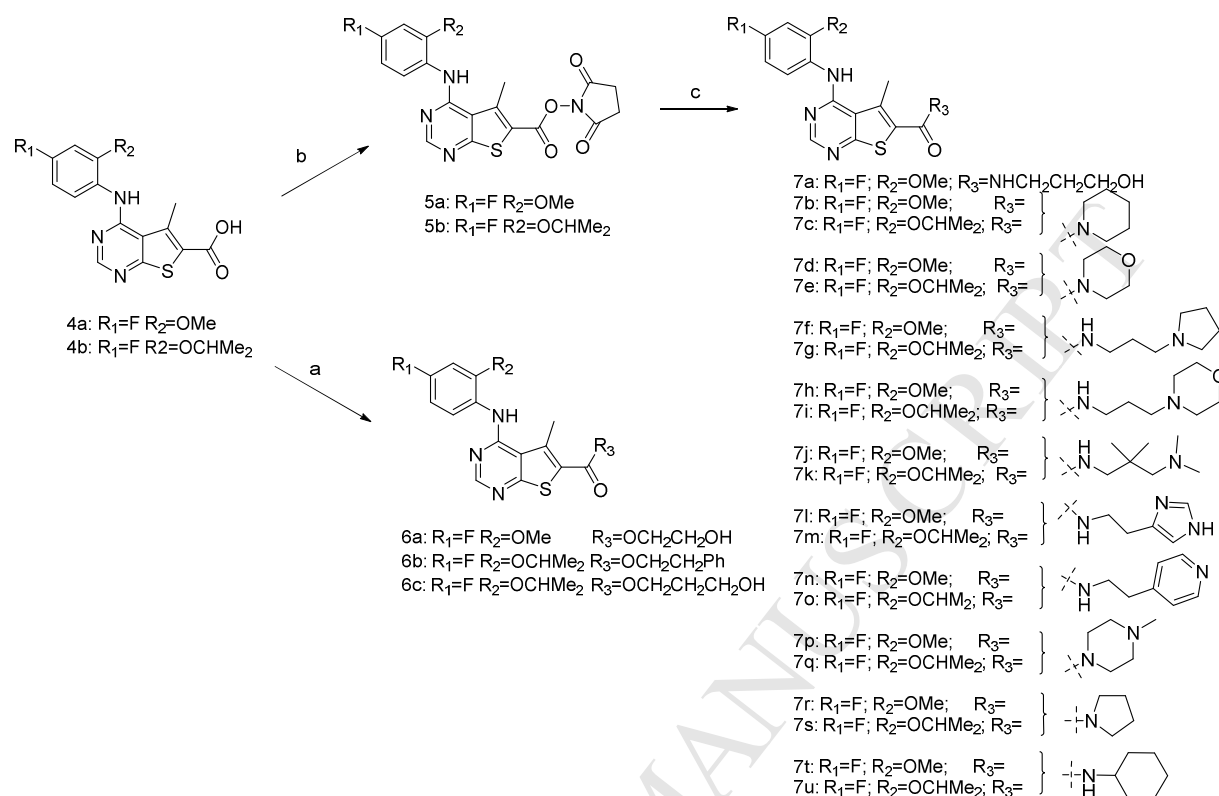
2.2 Synthesis of compounds

The reported synthetic routes for derivatives of the thieno[2,3-d]pyrimidine moiety of MNK-II [25, 26] suffer from several drawbacks. We have improved the routes to obtain a series of derivatives of *N*-(3-(dimethylamino)propyl)-4-((4-fluoro-2-((1-fluoropropan-2-yl)oxy)phenyl)amino)-5-methylthieno[2,3-d]pyrimidine-6-carboxamide. 5-Fluoro-2-nitrophenol was converted to 4-fluoro-2-isopropoxy-1-nitrobenzene by reacting with 2-bromopropane in the presence of potassium carbonate (K_2CO_3) in dimethylformamide (DMF) resulting in a yield of 70%. 4-Fluoro-2-isopropoxy-1-nitrobenzene and commercially available 4-fluoro-2-methoxy-1-nitrobenzene were hydrogenated over Pb/C under hydrogen gas to generate **2a** and **2b** (Scheme 1), followed by coupling with **1** which was synthesized as previously reported [26] using *N,N*-diisopropylethylamine (DIPEA) in isopropyl alcohol to obtain **3a**, **3b** respectively. Basic hydrolysis of the methyl ester group of **3a**, **3b** was carried out using $LiOH \cdot H_2O$ in a (1:1) mixture of tetrahydrofuran and water to produce **4a**, **4b** respectively (Scheme 2). Subsequent treatment of the carboxylic acids **4a**, **4b** with *N*-hydroxysuccinimide (NHS) and 1-ethyl-3-(3-dimethylaminopropyl)carbodiimide (EDCI) in DMF yielded **5a**, **5b**.



Scheme 1. Synthesis of Compounds 4a and 4b. Reagents and conditions: (a) DIPEA, 85°C, IPA, N₂, 10 h, 63% (**3a**), 85% (**3b**). (b) THF/H₂O; LiOH·H₂O, 2 M HCl, 84% (**4a**), 90% (**4b**).

The intermediates **5a** and **5b** can be stored stably at room temperature. A series of derivatives of MNK-II were obtained by reacting **5a** or **5b** with corresponding amine in DMF, followed by the addition of water to collect the precipitate, which was recrystallized in tetrahydrofuran (THF) and ether to yield **7a-t** or **7u** (Scheme 2) respectively. This synthetic method simplified the purification and preparation of the compound. We converted **4a** and **4b** to their corresponding esters (**6a**, **6b** and **6c**), by reacting with 2-phenylethyl bromide or 3-bromo-1-propanol or 2-bromoethanol in the presence of potassium carbonate (K₂CO₃) in DMF, respectively (Scheme 2).



Scheme 2. Synthesis of Compounds 6a-c, 7a-u. Reagents and conditions: (a) 2-bromoethanol, K_2CO_3 , DMF, 12 h, rt, 48% (**6a**); or 2-phenylethylbromide, K_2CO_3 , DMF, 12 h, rt, 48% (**6b**); or 3-bromo-1-propanol, DMF, K_2CO_3 , 12 h, rt, 48% (**6c**); (b) DMF, EDCI, NHS, rt, 61% (**5a**), 74% (**5b**); (c) DMF, related amine; H_2O .

2.3 Biological activity of the new compounds against MNKs

Our initial analysis tested the full set of compounds at 3 μM , at which concentration MNK-I1 completely inhibits eIF4E phosphorylation in cells. Several compounds proved to be inactive or much less active at inhibiting MNK function than MNK-I1 (compounds **6b**, **7b-d**, **7p**, **7r** and **7t**) (Fig. 4A). Compounds **6c**, **7e**, **7q**, **7s** and **7u** showed only partial inhibition (Fig. 4A). The strongest inhibition was observed for **7a**, **7f-i**, **7k-7o** (Fig. 4A). None of the compounds affected

the total amount of eIF4E. We then tested a subset of the stronger inhibitors, **7g**, **7i**, **7k**, **7m** and **7o**, at lower concentrations, down to final concentrations of 0.1 μM . Only **MNK-7g** showed a level of potency similar to MNK-I1 (Fig. 4B).

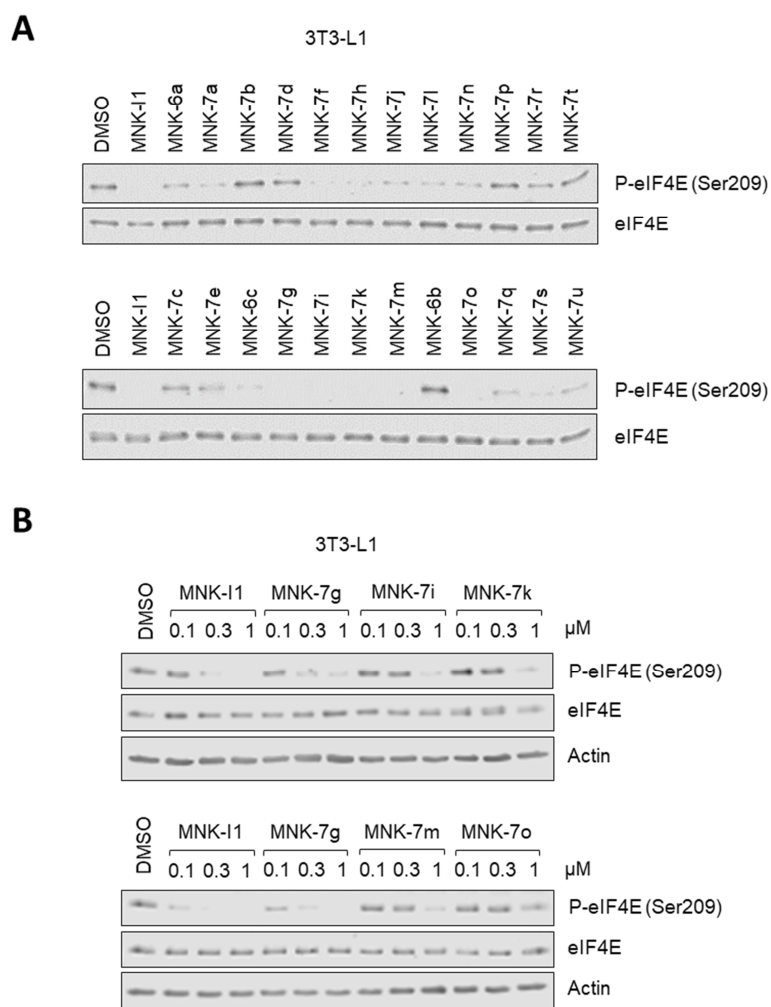


Figure 4. Evaluation of potential MNK inhibitors in 3T3-L1 cells. Mouse 3T3-L1 cells were treated with the indicated compounds at 3 μM (**A**) or at the concentrations shown (**B**), in each case for 2 h. As appropriate, the vehicle, DMSO, was used at a final concentration of 0.03-0.05%.

Cells were then lysed, and supernatants analysed by SDS-PAGE and western blot using the indicated antibodies.

The compound **MNK-7g** was docked *in silico* into the ATP binding site of MNK2 to explore the binding mode between the compound of **MNK-7g** and MNK2 (see Fig. 5A, B). From the interaction map, we observed some key features: two hydrogen bonds, with Met162 and Asn210, one ionic bond with Asp226, and a π -H stacking interaction with Leu90. The pattern of binding was similar to the interaction between staurosporine and MNK2, but with differences. Comparing the binding patterns of **MNK-7g** and MNK-I1 (Fig. 2B and Fig. 5B), we noticed that the location of the two compounds in the pocket was the same, with the distinction that they can form different hydrogen bonds to increase the stability of the binding to MNK2. The binding modes of the other two compounds (**7i** and **7o**) were similar to that of **MNK-7g** (see supplementary material Figure 1). We conclude that a bulky basic group at the C6-position might play a major role in the interaction with the MNKs and thus enhance the inhibition of MNKs and also improve the solubility to some extent. In contrast, when we changed the carbon chain, as in **7m** or **7u**, the inhibition became weaker than observed for MNK-I1 (Fig. 4A).

Compound **7s** clearly inhibited P-eIF4E less potently than **MNK-7g** (Fig. 4A). Therefore, **7s** was docked into the ATP binding site to assess differences in binding mode (see Fig. 5C, D). The binding map of **7s** showed that an ionic bond was formed between protonated N atom of pyrrolidine and negatively charged Asp226, but the hydrogen bond with Met162 was lost compared with the binding mode of **MNK-7g** (Fig. 5A, C). This indicated that a carbon chain of the appropriate length (two to three carbon atoms) can retain the hydrogen bond that the N atom of thienopyrimidine forms with Met162, which appeared important for the inhibitory activity of MNK2. When the amide bond (**7x** Fig. 3) was changed into an ester bond (**6c**), the compound's

inhibitory ability was almost unchanged. We speculated that the ester bond or amide bond had no obvious influence on the ability to inhibit the MNKs. However, when a polar substituent at the C6-position was replaced by a nonpolar group (compared **6d** and **6b**, seeing Fig. 3 and Scheme 2), inhibition of the MNKs was slightly weaker (Fig.3 and Fig. 4A), telling us that a polar substituent at C6-position was better. Thus, in terms of the compounds' structures, the N atom of the pyrimidine and a polar substituent group in the C6-position of thienopyrimidine appeared important for binding MNK2 and a substituent group at the C6-position of appropriate carbon chain length can enhance inhibition of the MNKs.

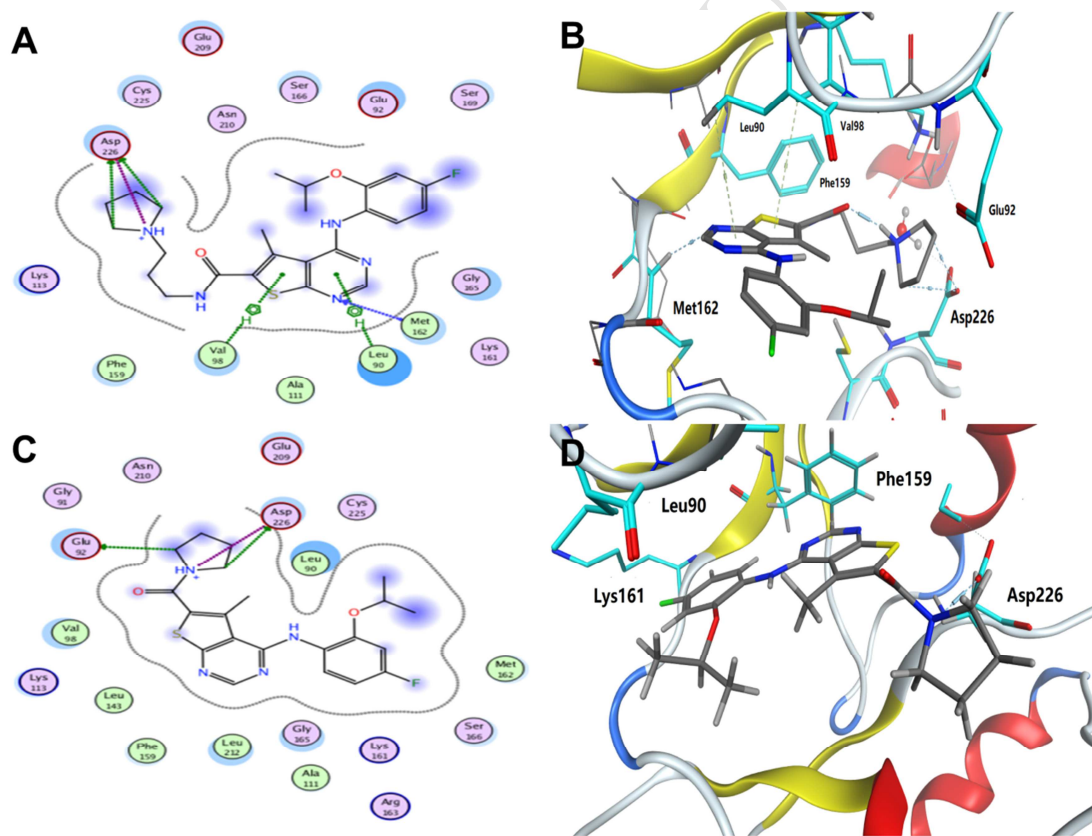


Figure 5. Comparison of the results between compounds **7g** and **7s** in the docking studies. (A) Interaction map, showing the binding between **7g** and MNK2. (B) The 3D combination mode of

7g and MNK2. (C) Interaction map, showing the binding pattern between **7s** and MNK2. (D) The 3D combination mode of **7s** and MNK2. Compounds are shown in stick representation: carbon in black, nitrogen in blue, oxygen in red, sulfur in yellow, and fluorine in green. Light blue depicts the amino acid residues in MNK2.

The compounds **7g**, **7i**, **7k**, **7m** and **7o** were more potent than **7f**, **7h**, **7j**, **7l** and **7n** in inhibiting MNK activity when the substituent group in the C6-position of thienopyrimidine was the same. This indicated that a bulky group in the *ortho*-position of the substituted aniline may increase the potency of MNK inhibition. Additionally, we found, by analysing the docking results of all compounds (Supplementary Material Figure 2), that the different substituent at the *ortho*-position of the substituted aniline can generate different interaction modes. Hence, we can infer that the group at the *ortho*-position of the substituted aniline group plays an important role in the ability of compounds to inhibit MNK activity.

2.4 Biological activity of compound MNK-7g

It was important to assess whether **MNK-7g** had affected any other major signaling pathways such as the ERK MAP kinase pathway (which is upstream of the MNKs), protein kinase B (also termed AKT) which mediates the effects of many stimuli, including insulin, and the mammalian target of rapamycin complex 1 (mTORC1) pathways, which exert manifold effects on gene expression, metabolism and cell growth.

In 3T3-L1 cells, MNK-I1 did not affect the phosphorylation (activation) of ERK, its downstream effector, the protein kinase RSK, or the phosphorylation of PKB, at Ser473, a substrate for mTOR complex 2 (Fig. 6A, quantified in Fig. 6B). MNK-I1 also did not affect the phosphorylation of 4E-BP1, a direct substrate for mTOR complex 1, or ribosomal protein (rp)

S6, an indirect target for mTORC1 signaling (Fig. 6A, B). These data are in close agreement with our earlier finding that MNK-I1 does not affect these pathways in human MDA-MB-231 cells [12]. However, they differ from the conclusions of Brown & Gromeier [35] who reported that MNKs promote mTORC1 activity under a specific condition (in response to insulin-like growth factor 1, IGF1). Our data suggested this is not a general effect as MNK inhibition clearly does not alter mTORC1 signaling here.

MNK-7g also did not affect phosphorylation of PKB, rpS6 or 4E-BP1 (Fig. 6A, B). However, interestingly, it did cause a slight increase in the phosphorylation of ERK and RSK perhaps by impairing a (so far hypothetical) inhibitory ‘loop’ linking the MNKs to their upstream activator, ERK.

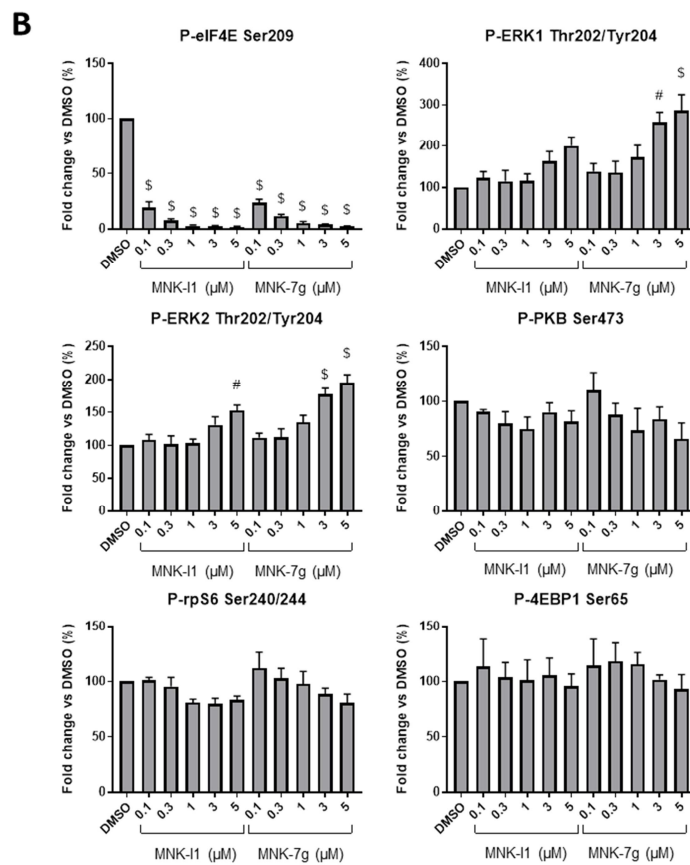
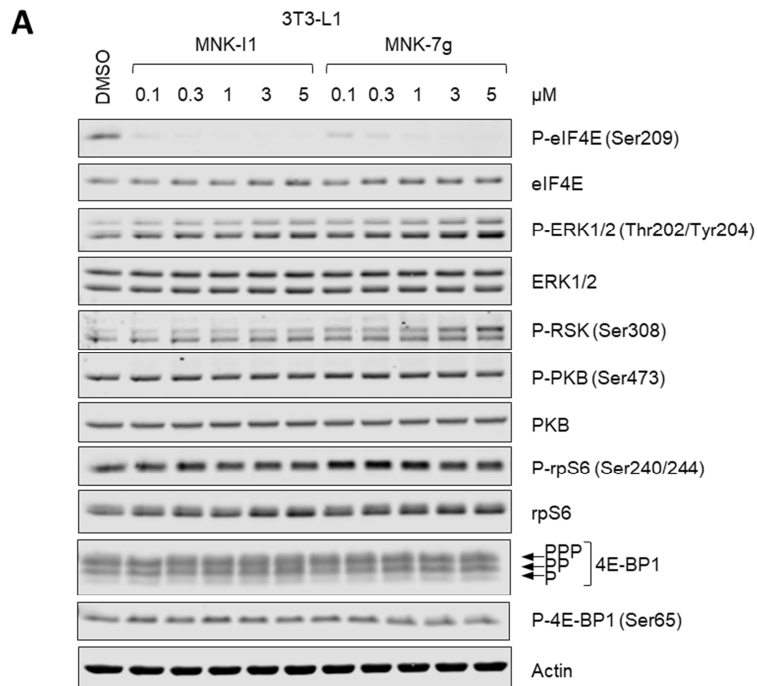


Figure 6. Comparison of the effects of MNK-I1 and **MNK-7g** on signaling pathways in 3T3-L1 cells. **(A)** 3T3-L1 cells were treated with the indicated compounds at the concentrations shown, in each case for 2 h. Cells were then lysed, and supernatants were analysed by SDS-PAGE and western blot using the indicated antibodies; for 4E-BP1, arrows show the differentially phosphorylated species, the top one (PPP) being the most highly phosphorylated one. **(B)** Quantification of data from three independent experiments for the indicated proteins. Error bars are SEM. \$ $p < 0.001$; # $p < 0.01$.

To assess the relative efficacy of MNK-I1 and **MNK-7g** against MNK1 and MNK2, we made use of cells (MEFs) from mice in which one or the other had been knocked out [10]. In wild-type MEFs, both MNK-I1 and **MNK-7g** each inhibited the phosphorylation of eIF4E completely at 5 μM and by 50% between 0.1 and 0.3 μM (Fig. 7A, B). In MNK1-KO cells, eIF4E phosphorylation reflects the activity of MNK2, and *vice versa* for MNK2-KO cells. Both compounds showed similar inhibition of P-eIF4E levels in MNK1-KO cells, with almost complete inhibition already seen at 0.1 μM (Fig. 7A). In contrast, at 0.3 μM , either compound only partially decreased P-eIF4E in MNK2-KO cells (Fig. 7A), 5 μM being needed to see inhibition similar to that observed with 0.1 μM in MNK1-KO cells. This indicated that both compounds inhibit MNK2 considerably more strongly than MNK1. To study their activities against MNK2 further, we treated MNK1-KO cells with even lower concentrations of MNK-I1 and **MNK-7g** (Fig. 7C; data quantified in 7D). **MNK-7g** showed slightly (roughly two-fold), and consistently, better potency against MNK2 than MNK-I1 (in MNK1-KO cells; Fig. 7D). Thus, both compounds are selective MNK2 inhibitors, with **MNK-7g** showing greater selectivity, i.e., slightly less inhibition of MNK1 and rather stronger inhibition of MNK2.

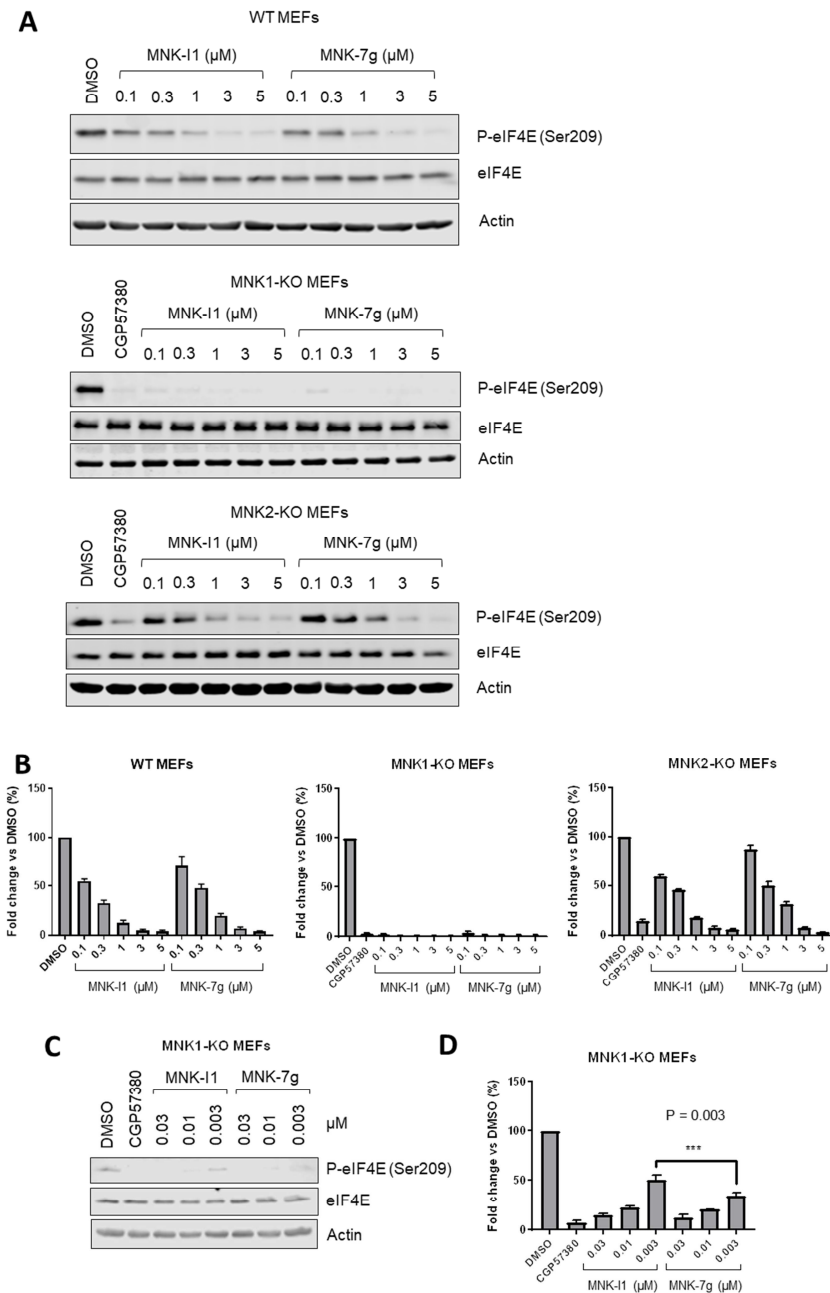


Figure 7. Comparison of the effects of MNK-I1 and **MNK-7g** on signaling pathways in wild-type and MNK knockout MEFs. **(A)** MEFs (wild-type, MNK1-KO or MNK2-KO, as shown) were treated with the indicated concentrations of MNK-I1 or **7g**, in each case for 2 h. CGP57380 was used at 50 μM . Cells were then lysed, and supernatants analysed by SDS-PAGE and western

blot using the indicated antibodies. **(B)** Quantification of data from three independent experiments for the indicated proteins. Error bars are SEM. **(C, D)** As **(A)**, but using lower inhibitor concentrations; **(D)** shows quantification of data from 3 independent experiments; ***, $p < 0.005$.

To further assess the relative efficiencies of MNK-I1 and **MNK-7g** against MNK1 and MNK2, we performed *in vitro* kinase assays using recombinant eIF4E as substrate, and MNK1 or MNK2 expressed in human embryonic kidney (HEK) 293 cells. Extensive pilot experiments were conducted to ensure that assays were within the linear range by adjusting the time of incubation, the amount of MNK1 or MNK2 and the quantity of eIF4E in the assays. The data clearly showed that **MNK-7g** and MNK-I1 had similar potencies against the two MNKs while, in agreement with the data for MNK-KO MEFs, **MNK-7g** was more effective than MNK-I1 against MNK2 (Fig. 8).

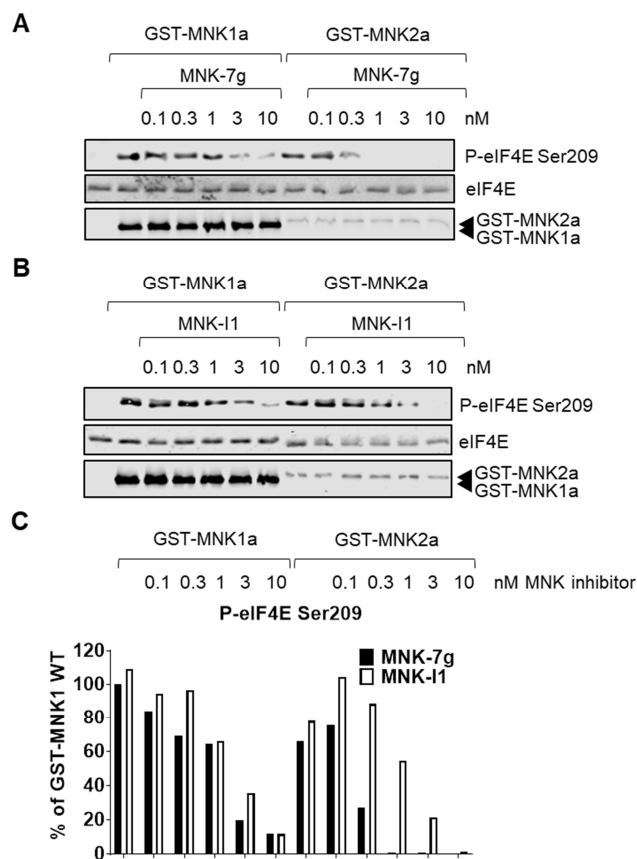


Figure 8. Inhibition of MNK-catalysed phosphorylation of eIF4E by MNK-I1 and **MNK-7g** *in vitro*. MNK assays were performed using recombinant GST-MNK1a and GST-MNK2a, with eIF4E as substrate, in the absence or presence of **MNK-7g** (in **A**) or MNK-I1 (in **B**) at the indicated concentrations. Reaction products were immunoblotted against for the indicated phospho- (P-) or total proteins. (**C**) Quantification of data from A and B. Similar data were obtained in a replicate experiment.

We extended the analysis of **MNK-7g** to a quite different cell type, (human) MDA-MB-231 breast cancer cells (Fig. 9A). The data showed that both **MNK-7g** and MNK-I1 decreased P-eIF4E levels in these cells, and caused almost complete inhibition at 1 μ M, confirming that they

are active against human MNKs. **MNK-7g** tended to be slightly less effective than MNK-I1 in these cells.

We have previously shown that MNK-I1 impairs the migration of MDA-MB-231 cells and other cancer cells [12]. As the migration assays need to be performed over a longer time-scale than the assays reported above (here, at least 48 h), it was important to assess whether the compounds were stable over this time period, i.e., they continued to block P-eIF4E. As shown in Fig. 9B, both MNK-I1 and **MNK-7g** still inhibited eIF4E phosphorylation at times beyond the length of the migration assay (up to 72 h), with only a slight tendency for P-eIF4E levels to rise at later times, especially in cells that received MNK-I1. This may suggest that MNK-I1 is less stable in aqueous solution at 37 °C than **MNK-7g**.

The effect of **MNK-7g** on cell migration was assessed using a 3-dimensional ‘Transwell’ assay, where it proved to be at least as effective as MNK-I1 in blocking the migration of MDA-MB-231 cells (Fig. 9C). **MNK-7g** did not effect on the distribution of cells in different phases of the cell cycle, as assessed by staining cells with propidium iodide followed by FACS analysis (Fig. 9D). There was also no change in the proportion of ‘sub G0’ cells indicating **MNK-7g** did not adversely affect cell viability. Since MNK inhibition does not affect the proliferation or cell cycle distribution of MDA-MB-231 cells (Fig. 9D and ref. [12]), the effects on migration cannot be a secondary consequence of reduced cell number (proliferation).

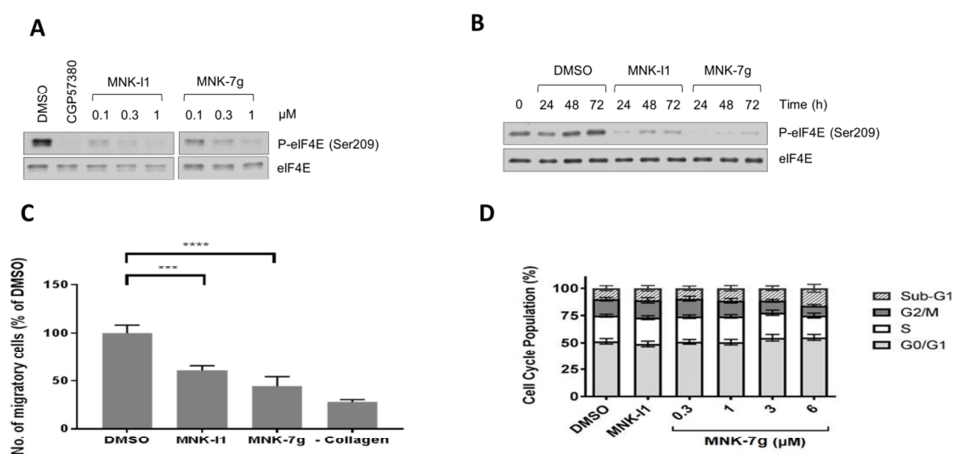


Figure 9. Effects of MNK-I1 and **MNK-7g** on the migration and proliferation of MDA-MB-231 breast cancer cells. **(A)** MDA-MB-231 cells were treated with the indicated concentrations of MNK-I1 or **7g**, in each case for 2 h. Cells were then lysed, and supernatants analysed by SDS-PAGE and western blot using the indicated antibodies. CGP57380 was used at 30 μ M. **(B)** MDA-MB-231 cells were treated with MNK-I1 or **MNK-7g** (3 μ M) for the indicated times, and samples were analysed as in **(A)**. **(C)** Transwell migration assays were performed with collagen as the attractant. After 24 h, the cells that had migrated were counted. Assays were performed in triplicate and data are shown \pm SEM; ***, $p < 0.005$; ****, $p < 0.001$. **(D)** Cell cycle analysis of MDA-MB-231 cells treated with 3 μ M MNK-I1 or the indicated concentrations of **MNK-7g**. Proportion (%) of cells at different stages of the cell cycle are displayed. Data are mean \pm SEM (n=5).

3. CONCLUSIONS

Using molecular docking and a structure-based design approach, we have achieved several improvements to the structure of inhibitors containing a thieno[2,3-d]pyrimidine scaffold that enhance MNK inhibition and simplify the synthetic route.

We designed and synthesized a series of MNK1 and/or MNK2 inhibitors containing a thieno[2,3-d]pyrimidine scaffold. Our studies revealed that polar substituent groups at the C6-position of thienopyrimidine with chain lengths of two to three carbons increase the binding efficiency and thus inhibition of the MNKs, whilst bulky groups in the *ortho*-position of the substituted aniline can increase the potency of MNK inhibition. Our docking studies pointed to two binding interactions that are important for MNK inhibition, i.e., one hydrogen bond with Met162 from the hinge region and another hydrogen bond with Asp226 from the DFD motif.

Our study also showed that the fluorinated isopropyl ether group at the *ortho*-position of the fluoroaniline group can be substituted with an isopropyl ether group without diminishing inhibitory activity. This modification is a practical way to simplify the synthetic route.

Another of our aims was to design and test compounds with greater selectivity towards MNK2. We found that one such compound, **MNK-7g**, possessed similar potency and somewhat greater selectivity to MNK2 when compared to MNK-I1. Importantly, **MNK-7g** did not affect any major signaling pathways other than a slight increase in the phosphorylation of ERK and RSK.

Given the simplified synthetic route, high yield and good stability, compound **MNK-7g** has been selected as a starting-point to develop further compounds suitable for probing the roles of MNK2 in cancer and especially in metabolic disease. This is the focus of ongoing efforts.

4. EXPERIMENTAL SECTION

4.1 Materials and chemicals

All cell culture solutions and supplements were purchased from Life Technologies unless indicated otherwise. Reagents for SDS-PAGE were purchased from Bio-Rad and Sigma. The Mnk inhibitor CGP57380 was obtained from Abcam.

4.2 Cell culture and treatment

3T3-L1 pre-adipocytes were maintained in Dulbecco's Modified Eagle's Medium (DMEM) high glucose with pyruvate (Cat. 11995-065) supplemented with 10% (v/v) fetal bovine serum (FBS) (Ausgenex; Lot. FBS00211-1; heat-inactivated at 55°C for 30 min) and 1% penicillin-streptomycin (P/S). Cells were strictly sub-cultured at 75-80% confluence every 2-3 days.

Mouse embryonic fibroblasts (MEFs) were prepared from E13.5 embryos of C57BL/6J mice in which the genes for MNK1 or MNK2 had been homozygously knocked out [17]. MEFs were maintained in DMEM (11995-065) supplemented with 10% (v/v) FBS and 1% P/S.

MDA-MB-231 cells were propagated as described previously [12].

All cells were maintained at 37°C in humidified air with 5% CO₂. Chemical treatments were added to the medium in DMSO vehicle at the appropriate concentrations for the indicated times (always <0.05% v/v DMSO).

4.3 SDS-PAGE and Western blot

Cell monolayers were harvested in RIPA lysis buffer containing 50 mM Tris-HCl, pH 7.5, 150 mM NaCl, 1% NP-40 (IGEPAL CA-630), 1% sodium deoxycholate, 0.1% sodium dodecyl

sulfate (SDS), 1 mM ethylenediaminetetraacetic acid (EDTA), 50 mM β -glycerophosphate, 0.5 mM NaVO_3 , 0.1% 2-mercaptoethanol and protease inhibitors (Roche). After lysis, insoluble material was removed by centrifugation at $>12,000$ g for 10 min at 4°C . Protein content was determined by the Bradford protein assay (Bio-Rad) [17]. Cell lysates were heated in sample buffer [250 mM Tris-HCl, 10% (v/v) sodium dodecyl sulfate (SDS), 20% (v/v) glycerol, 0.12% (w/v) bromophenol blue] at 95°C for 5 min and equal amounts of protein were then subjected to polyacrylamide gel electrophoresis (PAGE) and electrophoretic transfer to nitrocellulose membranes. Membranes were blocked in phosphate-buffered saline (PBS)-0.05% Tween20 containing 5% (w/v) skim milk powder for 30 min at room temperature. Membranes were probed with the indicated primary antibody overnight at 4°C . After incubation with fluorescently tagged secondary antibody, blots were visualised using a LI-COR Odyssey Quantitative Imaging System. Primary antibodies were from Cell Signaling Technology, except: P-eIF4E (Life Technologies), rpS6 (Santa Cruz) and actin (Sigma). Secondary antibodies were obtained from Fisher Scientific and used at 1:20,000 dilution.

4.4 *In vitro* MNK assays

MNK assays were performed as previously described [36]. Briefly, recombinant glutathione S-transferase (GST)-MNK fusion proteins GST-MNK1a and GST-MNK2a were purified by glutathione pull-down from lysates of transfected HEK293 cells. Recombinant GST-MNK were incubated in kinase assay buffer (25 mM Tris-HCl, pH7.5, 50 mM KCl and 2 mM MgCl_2) with 20 μM ATP and 65 ng eIF4E (expressed in *E. coli*) as substrate at 30°C for 30 min in the absence or presence of MNK inhibitors at indicated concentrations. Reactions were stopped by the addition of the above sample buffer, products were analysed by SDS-PAGE/immunoblotting using antisera against phosphorylated (P-) eIF4E Ser209, eIF4E and GST.

4.5 Cell migration assays

As previously described [12], for migration assays, Transwells (8 μm pore size, BD Biosciences) were pre-coated with 10 $\mu\text{g}/\text{ml}$ collagen (Millipore). Cells were pre-treated with inhibitors for 60 min before seeding at 3×10^5 into the Transwell inserts. Cells that had migrated into the bottom well after 24h were stained with DAPI (4',6-diamidino-2-phenylindole, 1:20,000) and visualized with a Nikon Eclipse Ni microscope ($\times 10$ objective lens). DAPI-stained cell numbers were quantified using ImageJ.

4.6 Cell cycle analysis

Cell cycle analysis utilised the propidium iodide staining method [37]. Briefly, MDA-MB-231 cells were seeded at 5×10^5 cells/well (6-well plate), given 24 h to attach and then treated with indicated amounts of inhibitor or vehicle. Cells were harvested at ~70% confluence and fixed in methanol for at least 2 h. Cells were centrifuged, resuspended in PBS and stained with 1 $\mu\text{g}/\text{ml}$ propidium iodide (PI). Roughly 20,000 PI-stained cells were analysed using a BD FACSCanto II flow cytometer. The data was analysed using BD FACSDiva software (BD Biosciences).

4.7 Statistics

Data were analysed by one-way ANOVA with Dunnett's multiple comparisons test for significance [12]. For the MNK1-KO MEF low dosage experiment, Sidak's multiple comparisons test for significance was used to compare the means of pairs of columns. For the cell cycle analysis, a two-way ANOVA with Tukey's multiple comparisons test was used. All statistical analyses were performed using GraphPad Prism 7 software.

4.8 Molecular docking

Molecular docking was performed using MOE with AMBER10: EHT forcefield [30]. The crystal structure of MNK2 was selected and downloaded from the Protein DataBank (PDB, <http://www.rcsb.org>), and was used for docking. The induced-fit docking approach was applied with consideration of the side chain flexibility of residues at the binding site. The ligand binding site was defined using the bound ligands in the crystal structures. The best scored conformation with minimum binding energy from the ten docking conformations of the ligands was selected for analysis.

4.9 Materials and general methods for synthetic chemistry

All starting materials and solvents were obtained from commercial sources and used without further purification. All actions were carried out with continuous magnetic stirring in common glassware and heating of reactions was performed with an IKA[®] heating block. Cooling of reactions was conducted with ice or an ice bath. pH was measured by Acidimeter. Thin-layer chromatography (TLC) was performed on precoated silica-gel 60 F254 plates (E. Merck). Column chromatography was performed on silica gel (200-300 mesh, Qingdao Marine Chemical Company, Qingdao, China). Melting points were determined on a Mitamura-Riken micro-hot stage and not corrected. ¹H NMR and ¹³C NMR spectra were obtained on a Bruker 500 NMR spectrometer (¹H at 500 MHz and ¹³C at 126 MHz) with tetramethylsilane (Me₄Si) as the internal standard. Chemical shifts are reported as δ values. Mass spectra were recorded on a Q-TOF Global mass spectrometer. The docking software was MOE (Molecular Operating Environment). The important intermediate methyl 4-chloro-5-methylthieno[2,3-d]pyrimidine-6-carboxylate (**1**) was synthesized as reported [26].

4.9.1 General procedure for purity determination by HPLC

An Agilent 1260 HPLC system (Agilent Technologies, Palo Alto, CA, USA) comprised a quaternary solvent delivery system, an on-line degasser, an auto-sampler, a column temperature controller and DAD detector coupled with an analytical workstation. The column configuration was an COSMOSIL C8 reserved phase column (5 μm , 250 mm \times 4.6 mm). The compounds were dissolved in methanol (compounds **6a**, **7b**, **7d** and **7e** were dissolved in THF) and injection volume was 10 μl . Detection wavelength was set at 254 nm, the flow rate was 1.0 ml min⁻¹ and the column temperature was maintained at 30°C. The mobile phase was elution solution which was mixed with solvent A (H₂O/0.1% TFA) and B (methanol) [25]. The mobile phase was gradient elution program which was as follows: 0-30 min, A: 80-0%, B: 20-100%. Results indicated that all the compounds used had a purity of more than 95%.

4.9.2 2, 5-dioxopyrrolidin-1-yl-4-((4-fluoro-2-methoxyphenyl)amino)-5-methylthieno[2,3-d]pyrimidine-6-carboxylate (**5a**).

A mixture of **4a** (400 mg, 1.2 mmol), EDCI (460 mg, 2.4 mmol), and NHS (276.22 mg, 2.4 mmol) in DMF (30 ml) was stirred at room temperature overnight. After the reaction was judged complete by TLC, the reaction mixture was diluted with water and extracted with ethyl acetate (20 ml) three times. The combined organic layers were washed with water and brine, dried over anhydrous MgSO₄, filtered, and concentrated *in vacuo*. The crude product was purified by chromatography (PE:EA = 2:1) to yield **5a** as a green powder (264 mg, 51%). ¹H NMR (500 MHz, CDCl₃) δ (ppm) : 8.68 (dd, J = 9.0, 6.2 Hz, 1H, benzene-H), 8.65 (s, 1H, pyrimidine-H), 8.27 (s, 1H, pyrimidine-NH-benzene), 6.78 (td, J = 8.8, 2.6 Hz, 1H, benzene-H), 6.72 (dd, J = 9.9, 2.5 Hz, 1H, benzene-H), 3.96 (s, 3H, OCH₃), 3.13 (s, 3H, thiophene-CH₃), 2.93 (s, 4H, succinimide-(CH₂)₂). ¹³C NMR (126 MHz, CDCl₃) δ (ppm): 168.9, 168.7, 159.3 (d, $J_{\text{C-F}}$ = 244 Hz), 158.1, 156.6, 156.5, 149.7 (d, $J_{\text{C-F}}$ = 9.9 Hz), 142.6, 123.7 (d, $J_{\text{C-F}}$ = 3.3 Hz), 122.2 (d, $J_{\text{C-F}}$ = 9.1

Hz), 117.5, 116.6, 106.9 (d, $J_{C-F} = 21.7$ Hz), 98.9 (d, $J_{C-F} = 27.4$ Hz), 56.4, 25.7, 16.2. HRMS calculated for (M+H)⁺ 431.0820, found 431.0820.

4.9.3 2,5-dioxopyrrolidin-1-yl-4-((4-fluoro-2-isopropoxyphenyl)amino)-5-methylthieno[2,3-d]pyrimidine-6-carboxylate (**5b**)

A mixture of **4b** (500 mg, 1.38 mmol), EDCI (530.8 mg, 2.77 mmol), and NHS (319 mg, 2.77 mmol) in DMF (30 ml) was stirred at room temperature overnight. After the reaction was judged complete by TLC, the reaction mixture was diluted with water and extracted with ethyl acetate (20 ml) three times. The combined organic layers were washed with water and brine, dried over anhydrous MgSO₄, filtered, and concentrated *in vacuo*. The crude product was purified by chromatography (PE:EA = 2:1) to yield **5b** as a green powder (500 mg, 79%). $R_f = 0.45$ (PE:EA = 2:1). ¹H NMR (500 MHz, CDCl₃) δ (ppm): 8.79 (dd, $J = 9.0, 6.3$ Hz, 1H, benzene-H), 8.66 (s, 1H, pyrimidine-H), 8.43 (s, 1H, pyrimidine-NH-benzene), 6.75 (td, $J = 8.6, 2.5$ Hz, 1H, benzene-H), 6.70 (dd, $J = 10.1, 2.6$ Hz, 1H, benzene-H), 4.71 - 4.63 (m, 1H, OCH(CH₃)₂), 3.15 (s, 3H, thiophene-CH₃), 2.92 (s, 4H, succinimide-(CH₂)₂), 1.43 (d, $J = 6.0$ Hz, 6H). ¹³C NMR (126 MHz, CDCl₃) δ (ppm): 168.9, 168.8, 159.1 (d, $J_{C-F} = 230.2$ Hz), 158.1, 156.5, 156.4, 147.5 (d, $J_{C-F} = 9.9$ Hz), 142.5, 124.6 (d, $J_{C-F} = 2.8$ Hz), 121.8 (d, $J_{C-F} = 9.1$ Hz), 117.6, 116.5, 106.7 (d, $J_{C-F} = 21.7$ Hz), 100.3 (d, $J_{C-F} = 27$ Hz), 71.8, 29.7, 25.6, 22.1, 16.4. HRMS calculated for (M+H)⁺ 459.1133, found 459.1132.

4.9.4 2-hydroxyethyl 4-((4-fluoro-2-methoxyphenyl)amino)-5-methylthieno[2,3-d]pyrimidine-6-carboxylate (**6a**)

A mixture of **4a** (100 mg, 0.276 mmol) and anhydrous K₂CO₃ (76.17 mg, 0.552 mmol) in DMF (10 ml) was stirred at room temperature for 1 h. And then 2-bromoethanol (249 μ l, 2.76

mmol) was added. The reaction was stirred at room temperature overnight. After the reaction was judged complete by TLC, the reaction mixture was diluted with water and extracted with ethyl acetate (20 ml) three times. The combined organic layers were washed with water and brine, dried over anhydrous MgSO_4 , filtered, and concentrated *in vacuo*. The crude product was purified by chromatography (PE:EA = 2:1) to yield **6a** as a white powder (56 mg, 48%). Melting point: 206°C - 208°C. ^1H NMR (500 MHz, $\text{DMSO-}d_6$) δ (ppm): 8.49 (s, 1H, pyrimidine-H), 8.45 (s, 1H, pyrimidine-NH-benzene), 8.15 (dd, $J = 8.8, 6.5$ Hz, 1H, benzene-H), 7.07 (dd, $J = 10.7, 2.7$ Hz, 1H, benzene-H), 6.84 (td, $J = 8.7, 2.7$ Hz, 1H, benzene-H), 4.93 (t, $J = 5.4$ Hz, 1H, $\text{CH}_2\text{CH}_2\text{OH}$), 4.31 (t, $J = 4.9$ Hz, 2H, OCH_2CH_2), 3.87 (s, 3H, OCH_3), 3.70 (q, $J = 5.2$ Hz, 2H, OCH_2CH_2), 3.06 (s, 3H, thiophene- CH_3). ^{13}C NMR (126 MHz, $\text{DMSO-}d_6$) δ (ppm): 167.1, 162.7, 160.0 (d, $J_{\text{C-F}} = 241.2$ Hz), , 157.3, 155.8, 152.7 (d, $J_{\text{C-F}} = 10.4$ Hz), 139.4, 124.8 (d, $J_{\text{C-F}} = 9.8$ Hz), 124.3 (d, $J_{\text{C-F}} = 2.9$ Hz), 122.3, 117.8, 106.6 (d, $J_{\text{C-F}} = 22$ Hz), 100.4 (d, $J_{\text{C-F}} = 27.2$ Hz), 67.5, 59.4, 57.0, 15.9. HRMS calculated for $(\text{M}+\text{H})^+$ 378.0918, found 378.0919. HPLC purity: 99.5%; retention time: 23.94 min.

4.9.5 Phenethyl-4-((4-fluoro-2-isopropoxyphenyl)amino)-5-methylthieno[2,3-d]pyrimidine-6-carboxylate (**6b**)

A mixture of **4b** (50 mg, 0.138 mmol) and anhydrous K_2CO_3 (38.27 mg, 0.276 mmol) in DMF (10 ml) was stirred at room temperature for 1 h and then (2-bromoethyl)benzene (186 μl , 1.38 mmol) was added. The reaction was stirred at room temperature overnight. After the reaction was judged complete by TLC, the reaction mixture was diluted with water and extracted with ethyl acetate (20 ml) three times. The combined organic layers were washed with water and brine, dried over anhydrous MgSO_4 , filtered, and concentrated *in vacuo*. The crude product was purified by chromatography (PE:EA = 5:1) to yield **6b** as a white powder (31 mg, 48.4%).

Melting point: 175°C - 177°C. ¹H NMR (500 MHz, DMSO-*d*₆) δ (ppm): 8.57 (s, 1H, pyrimidine-H), 8.53 (dd, *J* = 9.0, 6.5 Hz, 1H, benzene-H), 8.49 (s, 1H, pyrimidine-NH-benzene), 7.33 - 7.31 (m, 4H, benzene-H), 7.25 - 7.21 (m, 1H, benzene-H), 7.10 (dd, *J* = 10.8, 2.5 Hz, 1H, benzene-H), 6.82 (td, *J* = 8.8, 2.6 Hz, 1H, benzene-H), 4.82-4.76 (m, 1H, OCH(CH₃)₂), 4.51 (t, *J* = 6.6 Hz, 2H, OCH₂CH₂), 3.03 (t, *J* = 5.7 Hz, 2H, OCH₂CH₂), 3.01 (s, 3H, thiophene-CH₃), 1.31 (d, *J* = 6.0 Hz, 6H, OCH(CH₃)₂). ¹³C NMR (126 MHz, CDCl₃) δ (ppm): 167.5, 162.7, 158.8 (d, *J*_{C-F} = 242.8 Hz), 156.3, 155.5, 147.4 (d, *J*_{C-F} = 9.8 Hz), 137.6, 137.5, 129.0, 128.6, 126.7, 125.0 (d, *J*_{C-F} = 3.1 Hz), 123.2, 121.5 (d, *J*_{C-F} = 9.0 Hz), 117.9, 106.6 (d, *J*_{C-F} = 21.6 Hz), 100.3 (d, *J*_{C-F} = 27.1 Hz), 71.7, 65.9, 35.2, 22.1, 15.8. HRMS calculated for (M+H)⁺ 466.1595, found 466.1595.

4.9.6 3-hydroxypropyl-4-((4-fluoro-2-isopropoxyphenyl)amino)-5-methylthieno[2,3-*d*]pyrimidine-6-carboxylate (**6c**)

A mixture of **4b** (100 mg, 0.276 mmol) and anhydrous K₂CO₃ (76.17 mg, 0.552 mmol) in DMF (10 ml) was stirred at room temperature for 1 h. And then 3-bromo-1-propanol (249 μl, 2.76 mmol) was added. The reaction was stirred at room temperature overnight. After the reaction was judged complete by TLC, the reaction mixture was diluted with water and extracted with ethyl acetate (20 ml) three times. The combined organic layers were washed with water and brine, dried over anhydrous MgSO₄, filtered, and concentrated *in vacuo*. The crude product was purified by chromatography (PE:EA = 2:1) to yield **6c** as a white powder (56 mg, 48%). Melting point: 170°C - 172°C. ¹H NMR (500 MHz, DMSO-*d*₆) δ 8.56 (s, 1H, pyrimidine-H), 8.53 (dd, *J* = 9.0, 6.5 Hz, 1H, benzene-H), 8.49 (s, 1H, pyrimidine-NH-benzene), 7.09 (dd, *J* = 10.8, 2.6 Hz, 1H, benzene-H), 6.82 (td, *J* = 8.8, 2.6 Hz, 1H, benzene-H), 4.82 - 4.75 (m, 1H, OCH(CH₃)₂), 4.61 (t, *J* = 5.1 Hz, 1H, CH₂CH₂CH₂OH), 4.35 (t, *J* = 6.4 Hz, 2H, CH₂CH₂CH₂OH), 3.55 (q, *J* = 6.0 Hz, 2H, CH₂CH₂CH₂OH), 3.08 (s, 3H, thiophene-CH₃), 1.85 (p, *J* = 6.3 Hz, 2H,

CH₂CH₂CH₂OH), 1.32 (d, $J = 6.0$ Hz, 6H, OCH(CH₃)₂). ¹³C NMR (126 MHz, CDCl₃) δ (ppm): 167.4, 163.1, 158.8 (d, $J_{C-F} = 242.9$ Hz), 156.3, 155.6, 147.4 (d, $J_{C-F} = 9.6$ Hz), 137.9, 124.9 (d, $J_{C-F} = 2.9$ Hz), 122.9, 121.5 (d, $J_{C-F} = 8.9$ Hz), 117.9, 106.6 (d, $J_{C-F} = 21.6$ Hz), 100.3 (d, $J_{C-F} = 27.2$ Hz), 71.7, 62.2, 59.1, 31.7, 22.1, 15.8. HRMS calculated for (M+H)⁺ 420.1388, found 420.1389. HPLC purity: 95.5%; retention time: 29.67 min.

4.9.7 2-hydroxyethyl 4-((4-fluoro-2-isopropoxyphenyl)amino)-5-methylthieno[2,3-d]pyrimidine-6-carboxylate (**6d**)

Pale yellow powder (46.4%); melting point: 162°C - 164°C ¹H NMR (500 MHz, CDCl₃) δ 8.78 (dd, $J = 8.9, 6.4$ Hz, 1H, benzene-H), 8.61 (s, 1H, pyrimidine-H), 8.39 (s, 1H, pyrimidine-NH-benzene), 6.75 - 6.70 (m, 1H, benzene-H), 6.68 (dd, $J = 10.1, 2.3$ Hz, 1H, benzene-H), 4.70 - 4.61 (m, 1H, OCH(CH₃)₂), 4.50 - 4.46 (m, 2H, OCH₂CH₂), 4.01 - 3.95 (m, 2H, CH₂CH₂OH), 3.13 (s, 3H, thiophene-CH₃), 2.24 - 2.19 (m, 1H, CH₂CH₂OH), 1.43 (d, $J = 6.0$ Hz, 6H, OCH(CH₃)₂). ¹³C NMR (126 MHz, CDCl₃) δ 167.4, 163.0, 158.8 (d, $J_{C-F} = 242.9$ Hz), 156.3, 155.6, 147.4 (d, $J_{C-F} = 9.8$ Hz), 138.1, 124.9 (d, $J_{C-F} = 3.1$ Hz), 122.6, 121.5 (d, $J_{C-F} = 9.1$ Hz), 117.9, 106.6 (d, $J_{C-F} = 21.7$ Hz), 100.2 (d, $J_{C-F} = 27.1$ Hz), 71.7, 67.0, 61.2, 22.1, 15.8.

4.9.8 General procedure for **7a-7u**:

A mixture of **5a** or **5b** (1 equivalent) and the required amine (5 equivalent) in DMF (3 ml) was stirred at room temperature for 3 h. After being quenched with water, the mixture was filtered and the solid was washed with water and diethyl ether. Pure solid powder was obtained after recrystallization in THF/ diethyl ether (compounds **7a-7u**).

4.9.9 4-((4-fluoro-2-methoxyphenyl)amino)-N-(3-hydroxypropyl)-5-methylthieno[2,3-d]pyrimidine-6-carboxamide (**7a**)

Compound **7a** was prepared from 3-aminopropanol and **5a** using general procedure as a white solid in 37% yield. Melting point: 221°C - 224°C. ¹H NMR (500 MHz, DMSO-*d*₆) δ (ppm): 8.46 (s, 1H, pyrimidine-H), 8.41 (t, *J* = 5.4 Hz, 1H, CONH), 8.32 (s, 1H, pyrimidine-NH-benzene), 8.19 (dd, *J* = 8.8, 6.4 Hz, 1H, benzene-H), 7.07 (dd, *J* = 10.7, 2.7 Hz, 1H, benzene-H), 6.84 (td, *J* = 8.7, 2.7 Hz, 1H, benzene-H), 4.51 (t, *J* = 5.1 Hz, 1H, CH₂CH₂CH₂OH), 3.88 (s, 3H, OCH₃), 3.48 (q, *J* = 6.0 Hz, 2H, CH₂CH₂CH₂OH), 2.86 (s, 3H, thiophene-CH₃), 1.69 (p, *J* = 6.6 Hz, 2H, CH₂CH₂CH₂OH). (two hydrogens signal overlapping with water peak) ¹³C NMR (126 MHz, DMSO-*d*₆) δ (ppm): 165.8, 162.5, 159.8 (d, *J*_{C-F} = 240.8 Hz), 156.8, 154.7, 152.4 (d, *J*_{C-F} = 10.4 Hz), 131.0, 129.0, 124.5 (d, *J*_{C-F} = 3.0 Hz), 124.4 (d, *J*_{C-F} = 9.5 Hz), 117.4, 106.6 (d, *J*_{C-F} = 21.9 Hz), 100.4 (d, *J*_{C-F} = 27.2 Hz), 59.1, 57.1, 37.4, 32.7, 16.2. HRMS calculated for (M+H)⁺ 391.1235, found 391.1235. HPLC purity: 99.8%; retention time: 25.83 min.

*4.9.10 (4-((4-fluoro-2-methoxyphenyl)amino)-5-methylthieno[2,3-*d*]pyrimidin-6-yl)(piperidin-1-yl)methanone (7b)*

Compound **7b** was prepared from piperidine and **5a** using general procedure as a white solid in 37% yield. Melting point: 240°C - 241°C. ¹H NMR (500 MHz, DMSO-*d*₆) δ (ppm): 8.46 (s, 1H, pyrimidine-H), 8.25 (s, 1H, pyrimidine-NH-benzene), 8.22 (dd, *J* = 8.8, 6.4 Hz, 1H, benzene-H), 7.06 (dd, *J* = 10.7, 2.7 Hz, 1H, benzene-H), 6.84 (td, *J* = 8.7, 2.7 Hz, 1H, benzene-H), 3.88 (s, 3H, OCH₃), 3.67 - 3.35 (m, 4H, N-(CH₂)₂), 2.63 (s, 3H, thiophene-CH₃), 1.66 - 1.59 (m, 2H, (CH₂)₂-CH₂-(CH₂)₂), 1.57 - 1.48 (m, 4H, CH₂CH₂CH₂). ¹³C NMR (126 MHz, DMSO-*d*₆) δ (ppm): 166.4, 162.4, 160.6, 159.6 (d, *J*_{C-F} = 240.6 Hz), 156.5, 154.2, 152.2 (d, *J*_{C-F} = 10.4 Hz), 127.8, 127.7, 124.6 (d, *J*_{C-F} = 2.7 Hz), 124.0 (d, *J*_{C-F} = 9.6 Hz), 116.6, 106.6 (d, *J*_{C-F} = 22.2 Hz), 100.3 (d, *J*_{C-F} = 27.1 Hz), 57.1, 57.0, 24.3, 15.9. HRMS calculated for (M+H)⁺ 401.1442, found 401.1446. HPLC purity: 98.1%; retention time: 26.13 min.

4.9.11 (4-((4-fluoro-2-isopropoxyphenyl)amino)-5-methylthieno[2,3-d]pyrimidin-6-yl)(piperidin-1-yl)methanone (**7c**)

Compound **7c** was prepared from piperidine and **5b** using general procedure as a white solid in 80% yield. Melting point: 197°C - 198°C. ¹H NMR (500 MHz, DMSO-*d*₆) δ (ppm): 8.59 (dd, *J* = 9.0, 6.5 Hz, 1H, benzene-H), 8.53 (s, 1H, pyrimidine-H), 8.32 (s, 1H, pyrimidine-NH-benzene), 7.09 (dd, *J* = 10.8, 2.7 Hz, 1H, benzene-H), 6.82 (td, *J* = 8.8, 2.7 Hz, 1H, benzene-H), 4.83 - 4.74 (m, 1H, OCH(CH₃)₂), 3.67 - 3.35 (m, 4H, N-(CH₂)₂), 2.67 (s, 3H, thiophene-CH₃), 1.66 - 1.59 (m, 2H, (CH₂)₂-CH₂-(CH₂)₂), 1.56 - 1.48 (m, 4H, CH₂CH₂CH₂), 1.32 (d, *J* = 6.0 Hz, 6H, OCH(CH₃)₂). ¹³C NMR (126 MHz, DMSO-*d*₆) δ (ppm): 166.3, 162.3, 158.8 (d, *J*_{C-F} = 240.0 Hz), 155.8, 154.1, 148.5 (d, *J*_{C-F} = 10.3 Hz), 127.9, 127.6, 125.6 (d, *J*_{C-F} = 2.9 Hz), 121.9 (d, *J*_{C-F} = 9.5 Hz), 116.8, 106.4 (d, *J*_{C-F} = 21.7 Hz), 101.5 (d, *J*_{C-F} = 26.9 Hz), 71.8, 24.3, 22.1, 16.0. HRMS calculated for (M+H)⁺ 429.1755, found 429.1756. HPLC purity: 98.2%; retention time: 26.50 min.

4.9.12 (4-((4-fluoro-2-methoxyphenyl)amino)-5-methylthieno[2,3-d]pyrimidin-6-yl)(morpholino)methanone (**7d**)

Compound **7d** was prepared from morpholine and **5a** using general procedure as a white solid in 59% yield. Melting point: 237°C - 240°C. ¹H NMR (500 MHz, DMSO-*d*₆) δ (ppm): 8.46 (s, 1H, pyrimidine-H), 8.26 (s, 1H, pyrimidine-NH-benzene), 8.22 (dd, *J* = 8.8, 6.5 Hz, 1H, benzene-H), 7.07 (dd, *J* = 10.7, 2.6 Hz, 1H, benzene-H), 6.84 (td, *J* = 8.7, 2.7 Hz, 1H, benzene-H), 3.87 (s, 3H, OCH₃), 3.66 - 3.58 (m, 4H, (CH₂)₂O), 3.58 - 3.42 (m, 4H, N(CH₂)₂), 2.66 (s, 3H, thiophene-CH₃). ¹³C NMR (126 MHz, DMSO-*d*₆) δ (ppm): 166.6, 162.8, 159.6 (d, *J*_{C-F} = 240.8 Hz), 156.5, 154.3, 152.2 (d, *J*_{C-F} = 10.6 Hz), 128.5, 126.9, 124.6 (d, *J*_{C-F} = 3.1 Hz), 124.0 (d, *J*_{C-F}

= 9.6 Hz), 116.6, 106.6 (d, J_{C-F} = 21.9 Hz), 100.3 (d, J_{C-F} = 27.3 Hz), 66.6, 57.1, 16.0. HRMS calculated for (M+H)⁺ 403.1235, found 403.1235. HPLC purity: 95.1%; retention time: 22.52 min.

4.9.13 4-((4-fluoro-2-isopropoxyphenyl)amino)-5-methylthieno[2,3-d]pyrimidin-6-yl)(morpholino)methanone (**7e**)

Compound **7e** was prepared from morpholine and **5b** using general procedure as a white solid in 77% yield. Melting point: 227°C - 230°C. ¹H NMR (500 MHz, DMSO-*d*₆) δ (ppm): 8.60 (dd, J = 9.0, 6.5 Hz, 1H, benzene-H), 8.54 (s, 1H, pyrimidine-H), 8.34 (s, 1H, pyrimidine-NH-benzene), 7.09 (dd, J = 10.8, 2.7 Hz, 1H, benzene-H), 6.82 (td, J = 8.8, 2.7 Hz, 1H, benzene-H), 4.83 - 4.76 (m, 1H, OCH(CH₃)₂), 3.67 - 3.58 (m, 4H, (CH₂)₂O), 3.58 - 3.42 (m, 4H, N(CH₂)₂), 2.70 (s, 3H, thiophene-CH₃), 1.33 (d, J = 6.0 Hz, 6H, OCH(CH₃)₂). ¹³C NMR (126 MHz, DMSO-*d*₆) δ (ppm): 166.4, 162.8, 158.8 (d, J_{C-F} = 240.1 Hz), 155.9, 154.2, 148.5 (d, J_{C-F} = 10.2 Hz), 128.2, 127.1, 125.6 (d, J_{C-F} = 2.9 Hz), 121.9 (d, J_{C-F} = 9.4 Hz), 116.8, 106.4 (d, J_{C-F} = 22.0 Hz), 101.5 (d, J_{C-F} = 27.0 Hz), 71.8, 66.6, 22.1, 16.1. HRMS calculated for (M+H)⁺ 431.1548, found 431.1545. HPLC purity: 97.9%; retention time: 26.38 min.

4.9.14 4-((4-fluoro-2-methoxyphenyl)amino)-5-methyl-N-(3-(pyrrolidin-1-yl)propyl)thieno[2,3-d]pyrimidine-6-carboxamide (**7f**)

Compound **7f** was prepared from 1-(3-aminopropyl)pyrrolidine and **5a** using general procedure as a white solid in 48% yield. Melting point: 194°C - 197°C. ¹H NMR (500 MHz, DMSO-*d*₆) δ (ppm): 8.55 (t, J = 5.3 Hz, 1H, CONH), 8.46 (s, 1H, pyrimidine-H), 8.32 (s, 1H, pyrimidine-NH-benzene), 8.19 (dd, J = 8.6, 6.6 Hz, 1H, benzene-H), 7.07 (dd, J = 10.7, 2.6 Hz, 1H, benzene-H), 6.84 (td, J = 8.7, 2.6 Hz, 1H, benzene-H), 3.87 (s, 3H, OCH₃), 3.29 (d, J = 6.5

Hz, 2H, CONHCH₂), 2.87 (s, 3H, thiophene-CH₃), 2.48 - 2.40 (m, 6H, N(CH₂)₃), 1.73 - 1.65 (m, 6H, NHCH₂CH₂CH₂N, CH₂-(CH₂)₂-CH₂). ¹³C NMR (126 MHz, DMSO-*d*₆) δ (ppm): 165.8, 162.4, 159.8 (d, *J*_{C-F} = 240.8 Hz), 156.8, 154.7, 152.4 (d, *J*_{C-F} = 10.5 Hz), 131.3, 128.8, 124.5 (d, *J*_{C-F} = 2.3 Hz), 124.4 (d, *J*_{C-F} = 9.7 Hz), 117.5, 106.6 (d, *J*_{C-F} = 21.8 Hz), 100.4 (d, *J*_{C-F} = 27.1 Hz), 57.1, 54.1, 54.0, 38.9, 28.4, 23.6, 16.2. HRMS calculated for (M+H)⁺ 444.1864, found 444.1869. HPLC purity: 98.3%; retention time: 22.11 min.

4.9.15 4-((4-fluoro-2-isopropoxyphenyl)amino)-5-methyl-N-(3-(pyrrolidin-1-yl)propyl)thieno[2,3-*d*]pyrimidine-6-carboxamide (**7g**)

Compound **7g** was prepared from 1-(3-aminopropyl)pyrrolidine and **5b** using general procedure as a white solid in 89% yield. Melting point: 179°C. ¹H NMR (500 MHz, CDCl₃) δ (ppm): 8.91 (t, *J* = 4.7 Hz, 1H, CONH), 8.79 (dd, *J* = 9.0, 6.3 Hz, 1H, benzene-H), 8.59 (s, 1H, pyrimidine-H), 8.40 (s, 1H, pyrimidine-NH-benzene), 6.73 (td, *J* = 8.6, 2.7 Hz, 1H, benzene-H), 6.68 (dd, *J* = 10.2, 2.7 Hz, 1H, benzene-H), 4.70 - 4.62 (m, 1H, OCH(CH₃)₂), 3.57 (dd, *J* = 10.6, 5.6 Hz, 2H, CONHCH₂), 3.11 (s, 3H, thiophene-CH₃), 2.72 (t, *J* = 5.7 Hz, 2H, CH₂N), 2.60 (t, 4H, *J* = 6.5 Hz, N(CH₂)₂), 1.89 - 1.83 (m, 4H, CH₂-(CH₂)₂-CH₂), 1.83 - 1.77 (m, 2H, NHCH₂CH₂CH₂N), 1.42 (d, *J* = 6.1 Hz, 6H, OCH(CH₃)₂). ¹³C NMR (126 MHz, CDCl₃) δ (ppm): 165.6, 162.8, 158.7 (d, *J*_{C-F} = 242.3 Hz), 156.1, 154.8, 147.4 (d, *J*_{C-F} = 9.8 Hz), 132.8, 127.1, 125.2 (d, *J*_{C-F} = 3.1 Hz), 121.2 (d, *J*_{C-F} = 9.0 Hz), 118.3, 106.5 (d, *J*_{C-F} = 21.6 Hz), 100.2 (d, *J*_{C-F} = 27.0 Hz), 71.6, 56.4, 54.2, 41.6, 25.6, 23.7, 22.1, 15.9. HRMS calculated for (M+H)⁺ 472.2177, found 472.2178. HPLC purity: 98.6%; retention time: 21.87 min.

4.9.16 4-((4-fluoro-2-methoxyphenyl)amino)-5-methyl-N-(3-morpholinopropyl)thieno[2,3-*d*]pyrimidine-6-carboxamide (**7h**)

Compound **7h** was prepared from *N*-(3-aminopropyl)morpholine and **5a** using general procedure as a white solid in 75% yield. Melting point: 176°C. ¹H NMR (500 MHz, DMSO-*d*₆) δ (ppm): 8.48 - 8.43 (m, 2H, pyrimidine-H, CONH), 8.32 (s, 1H, pyrimidine-NH-benzene), 8.18 (dd, *J* = 8.8, 6.4 Hz, 1H, benzene-H), 7.07 (dd, *J* = 10.7, 2.7 Hz, 1H, benzene-H), 6.84 (td, *J* = 8.7, 2.7 Hz, 1H, benzene-H), 3.87 (s, 3H, OCH₃), 3.57 (t, *J* = 4.5 Hz, 4H, CH₂OCH₂), 3.30 - 3.25 (m, 2H, CONHCH₂), 2.86 (s, 3H, thiophene-CH₃), 2.39 - 2.30 (m, 6H, CH₂N(CH₂)₂), 1.69 (p, *J* = 7.0 Hz, 2H, NHCH₂CH₂CH₂N). ¹³C NMR (126 MHz, DMSO-*d*₆) δ (ppm): 165.8, 162.5, 159.8 (d, *J*_{C-F} = 240.6 Hz), 156.8, 154.7, 152.4 (d, *J*_{C-F} = 10.3 Hz), 131.2, 128.8, 124.5 (d, *J*_{C-F} = 3.2 Hz), 124.4 (d, *J*_{C-F} = 9.7 Hz), 117.5, 106.6 (d, *J*_{C-F} = 21.8 Hz), 100.3 (d, *J*_{C-F} = 27.1 Hz), 66.7, 57.1, 56.5, 53.8, 38.5, 26.2, 16.2. HRMS calculated for (M+H)⁺ 460.1813, found 460.1814. HPLC purity: 99.1%; retention time: 21.86 min.

4.9.17 4-((4-fluoro-2-isopropoxyphenyl)amino)-5-methyl-*N*-(3-morpholinopropyl)thieno[2,3-*d*]pyrimidine-6-carboxamide (**7i**)

Compound **7i** was prepared from *N*-(3-aminopropyl)morpholine and **5b** using general procedure as a white solid in 75% yield. Melting point: 162°C - 165°C. ¹H NMR (500 MHz, DMSO-*d*₆) δ (ppm): 8.57 (dd, *J* = 9.0, 6.4 Hz, 1H, benzene-H), 8.53 (s, 1H, pyrimidine-H), 8.48 (t, *J* = 5.5 Hz, 1H, CONH), 8.41 (s, 1H, pyrimidine-NH-benzene), 7.10 (dd, *J* = 10.8, 2.7 Hz, 1H, benzene-H), 6.82 (td, *J* = 8.7, 2.7 Hz, 1H, benzene-H), 4.83 - 4.76 (m, 1H, OCH(CH₃)₂), 3.57 (t, *J* = 4.5 Hz, 4H, CH₂OCH₂), 3.30 - 3.26 (m, 2H, CONHCH₂), 2.91 (s, 3H, thiophene-CH₃), 2.38 - 2.31 (m, 6H, CH₂N(CH₂)₂), 1.69 (p, *J* = 7.0 Hz, 2H, NHCH₂CH₂CH₂N), 1.32 (d, *J* = 6.0 Hz, 6H, OCH(CH₃)₂). ¹³C NMR (126 MHz, DMSO-*d*₆) δ (ppm): 165.7, 162.4, 158.9 (d, *J*_{C-F} = 239.9 Hz), 156.1, 154.7, 148.7 (d, *J*_{C-F} = 10.4 Hz), 130.9, 129.0, 125.5 (d, *J*_{C-F} = 2.5 Hz), 122.2 (d, *J*_{C-F} = 9.5 Hz), 117.6, 106.5 (d, *J*_{C-F} = 21.8 Hz), 101.5 (d, *J*_{C-F} = 26.9 Hz), 71.8, 66.7, 56.5, 53.8, 38.5, 26.2,

22.1, 16.3. HRMS calculated for (M+H)⁺ 488.2126, found 488.2127. HPLC purity: 99.5%; retention time: 21.78 min.

4.9.18 *N*-(3-(dimethylamino)-2,2-dimethylpropyl)-4-((4-fluoro-2-methoxyphenyl)amino)-5-methylthieno[2,3-*d*]pyrimidine-6-carboxamide (**7j**)

Compound **7j** was prepared from *N,N*,2,2-tetramethyl-1,3-propanediamine and **5a** using general procedure as a white solid in 39% yield. Melting point: 171°C - 174°C. ¹H NMR (500 MHz, DMSO-*d*₆) δ (ppm): 8.69 (t, *J* = 5.6 Hz, 1H, CONH), 8.46 (s, 1H, pyrimidine-H), 8.32 (s, 1H, pyrimidine-NH-benzene), 8.17 (dd, *J* = 8.9, 6.4 Hz, 1H, benzene-H), 7.07 (dd, *J* = 10.7, 2.7 Hz, 1H, benzene-H), 6.84 (td, *J* = 8.7, 2.7 Hz, 1H, benzene-H), 3.87 (s, 3H, OCH₃), 3.20 (d, *J* = 5.7 Hz, 2H, CONHCH₂), 2.88 (s, 3H, thiophene-CH₃), 2.26 (s, 6H, N(CH₃)₂), 2.20 (s, 2H, CH₂N(CH₃)₂), 0.90 (s, 6H, CH₂C(CH₃)₂CH₂). ¹³C NMR (126 MHz, DMSO-*d*₆) δ (ppm): 165.8, 162.7, 159.8 (d, *J*_{C-F} = 240.7 Hz), 156.8, 154.7, 152.5 (d, *J*_{C-F} = 10.5 Hz), 131.0, 129.2, 124.5 (d, *J*_{C-F} = 2.5 Hz), 124.5 (d, *J*_{C-F} = 9.5 Hz), 117.6, 106.6 (d, *J*_{C-F} = 21.8 Hz), 100.4 (d, *J*_{C-F} = 27.2 Hz), 69.4, 57.1, 49.3, 48.8, 36.8, 24.6, 16.2. HRMS calculated for (M+H)⁺ 446.2021, found 446.2021. HPLC purity: 98.5%; retention time: 22.21 min.

4.9.19 *N*-(3-(dimethylamino)-2,2-dimethylpropyl)-4-((4-fluoro-2-isopropoxyphenyl)amino)-5-methylthieno[2,3-*d*]pyrimidine-6-carboxamide (**7k**)

Compound **7k** was prepared from *N,N*,2,2-tetramethyl-1,3-propanediamine and **5b** using general procedure as a white solid in 70% yield. Melting point: 106°C. ¹H NMR (500 MHz, DMSO-*d*₆) δ (ppm): 8.72 (t, *J* = 5.5 Hz, 1H, CONH), 8.57 (dd, *J* = 9.0, 6.5 Hz, 1H, benzene-H), 8.54 (s, 1H, pyrimidine-H), 8.41 (s, 1H, pyrimidine-NH-benzene), 7.10 (dd, *J* = 10.8, 2.7 Hz, 1H, benzene-H), 6.82 (td, *J* = 8.7, 2.7 Hz, 1H, benzene-H), 4.83 - 4.75 (m, 1H, OCH(CH₃)₂), 3.20 (d,

$J = 5.6$ Hz, 2H, CONHCH₂), 2.93 (s, 3H, thiophene-CH₃), 2.26 (s, 6H, N(CH₃)₂), 2.21 (s, 2H, CH₂N(CH₃)₂), 1.32 (d, $J = 6.0$ Hz, 6H, OCH(CH₃)₂), 0.90 (s, 6H, CH₂C(CH₃)₂ CH₂). ¹³C NMR (126 MHz, DMSO-*d*₆) δ (ppm): 165.7, 162.6, 158.9 (d, $J_{C-F} = 239.9$ Hz), 156.1, 154.7, 148.7 (d, $J_{C-F} = 10.4$ Hz), 130.7, 129.4, 125.5 (d, $J_{C-F} = 2.6$ Hz), 122.2 (d, $J_{C-F} = 9.4$ Hz), 117.7, 106.5 (d, $J_{C-F} = 21.7$ Hz), 101.5 (d, $J_{C-F} = 27.0$ Hz), 71.8, 69.4, 49.4, 48.8, 36.8, 24.6, 22.1, 16.3. HRMS calculated for (M+H)⁺ 474.2334, found 474.2335. HPLC purity: 98.2%; retention time: 21.93 min.

4.9.20 *N*-(2-(1*H*-imidazol-4-yl)ethyl)-4-((4-fluoro-2-methoxyphenyl)amino)-5-methylthieno[2,3-*d*]pyrimidine-6-carboxamide (**7l**)

Compound **7l** was prepared from histamine and **5a** using general procedure as a white solid in 32% yield. Melting point: 264°C - 266°C. ¹H NMR (500 MHz, DMSO-*d*₆) δ (ppm): 11.83 (s, 1H, imidazole-NH), 8.53 (t, $J = 5.4$ Hz, 1H, CONH), 8.46 (s, 1H, pyrimidine-H), 8.32 (s, 1H, pyrimidine-NH-benzene), 8.18 (dd, $J = 8.8, 6.4$ Hz, 1H, benzene-H), 7.54 (s, 1H, imidazole-H), 7.07 (dd, $J = 10.7, 2.7$ Hz, 1H, benzene-H), 6.90 - 6.81 (m, 2H, benzene-H, imidazole-H), 3.88 (s, 3H, OCH₃), 3.48 (q, $J = 7.1$ Hz, 2H, CONHCH₂), 2.83 (s, 3H, thiophene-CH₃), 2.77 (t, $J = 6.4$ Hz, 2H, CH₂-imidazole). ¹³C NMR (126 MHz, DMSO-*d*₆) δ (ppm): 165.8, 162.4, 159.8 (d, $J_{C-F} = 241.0$ Hz), 156.8, 154.7, 152.5 (d, $J_{C-F} = 10.6$ Hz), 135.2, 131.2, 128.9, 125.5 (d, $J_{C-F} = 2.6$ Hz), 124.5 (d, $J_{C-F} = 9.5$ Hz), 117.5, 106.5 (d, $J_{C-F} = 21.7$ Hz), 101.5 (d, $J_{C-F} = 27.0$ Hz), 57.1, 27.2 16.2. HRMS calculated for (M+H)⁺ 427.1347, found 427.1345. HPLC purity: 98.9%; retention time: 18.36 min.

4.9.21 *N*-(2-(1*H*-imidazol-4-yl)ethyl)-4-((4-fluoro-2-isopropoxyphenyl)amino)-5-methylthieno[2,3-*d*]pyrimidine-6-carboxamide (**7m**)

Compound **7m** was prepared from histamine and **5b** using general procedure as a white solid in 80% yield. Melting point: 189°C - 191°C. ¹H NMR (500 MHz, DMSO-*d*₆) δ (ppm): 11.87 (s, 1H, imidazole-NH), 8.59 - 8.55 (m, 2H, CONH, benzene-H), 8.53 (s, 1H, pyrimidine-H), 8.41 (s, 1H, pyrimidine-NH-benzene), 7.55 (s, 1H, imidazole-H), 7.10 (dd, *J* = 10.8, 2.7 Hz, 1H, benzene-H), 6.85 (s, 1H, imidazole-H), 6.84 - 6.79 (m, 1H, benzene-H), 4.84 - 4.75 (m, 1H, OCH(CH₃)₂), 3.49 (q, *J* = 7.1 Hz, 2H, CONHCH₂), 2.87 (d, *J* = 8.6 Hz, 3H, thiophene-CH₃), 2.78 (t, *J* = 7.3 Hz, 2H, CH₂-imidazole), 1.32 (d, *J* = 6.0 Hz, 6H, OCH(CH₃)₂). ¹³C NMR (126 MHz, DMSO-*d*₆) δ (ppm): 165.7, 162.4, 158.9 (d, *J*_{C-F} = 240.2 Hz), 156.1, 154.7, 148.6 (d, *J*_{C-F} = 10.3 Hz), 135.2, 130.9, 129.2, 125.5 (d, *J*_{C-F} = 2.9 Hz), 122.2 (d, *J*_{C-F} = 9.4 Hz), 117.6, 106.5 (d, *J*_{C-F} = 21.8 Hz), 101.5 (d, *J*_{C-F} = 27.0 Hz), 71.8, 27.2, 22.2, 16.2. HRMS calculated for (M+H)⁺ 455.1660, found 455.1661. HPLC purity: 96.2%; retention time: 21.78 min.

4.9.22 4-((4-fluoro-2-methoxyphenyl)amino)-5-methyl-N-(2-(pyridin-4-yl)ethyl)thieno[2,3-*d*]pyrimidine-6-carboxamide (**7n**)

Compound **7n** was prepared from 4-(2-aminoethyl)pyridine and **5a** using general procedure as a white solid in 63% yield. Melting point: 225°C - 229°C. ¹H NMR (500 MHz, DMSO-*d*₆) δ (ppm): 8.52 (t, *J* = 5.5 Hz, 1H, CONH), 8.48 (d, *J* = 5.7 Hz, 2H, pyridine-H), 8.45 (s, 1H, pyrimidine-H), 8.30 (s, 1H, pyrimidine-NH-benzene), 8.16 (dd, *J* = 8.8, 6.4 Hz, 1H, benzene-H), 7.29 (d, *J* = 5.6 Hz, 2H, pyridine-H), 7.06 (dd, *J* = 10.7, 2.7 Hz, 1H, benzene-H), 6.84 (td, *J* = 8.7, 2.7 Hz, 1H, benzene-H), 3.87 (s, 3H, OCH₃), 3.54 (q, *J* = 6.8 Hz, 2H, CONHCH₂), 2.89 (t, *J* = 7.0 Hz, 2H, CH₂-pyridine), 2.76 (s, 3H, thiophene-CH₃). ¹³C NMR (126 MHz, DMSO-*d*₆) δ (ppm): 165.8, 162.6, 159.8 (d, *J*_{C-F} = 240.9 Hz), 156.8, 154.7, 152.5 (d, *J*_{C-F} = 10.5 Hz), 149.9, 148.7, 131.4, 128.5, 124.8, 124.5 (d, *J*_{C-F} = 10.1 Hz), 124.4 (d, *J*_{C-F} = 3.1 Hz), 117.4, 106.6 (d, *J*_{C-}

$f_F = 21.9$ Hz), 100.4 (d, $J_{C-F} = 27.1$ Hz), 57.0, 34.4, 16.1. HRMS calculated for $(M+H)^+$ 438.1395, found 438.1398. HPLC purity: 98.6%; retention time: 18.19 min.

4.9.23 4-((4-fluoro-2-isopropoxyphenyl)amino)-5-methyl-N-(2-(pyridin-4-yl)ethyl)thieno[2,3-d]pyrimidine-6-carboxamide (**7o**)

Compound **7o** was prepared from 4-(2-aminoethyl)pyridine and **5b** using general procedure as a white solid in 65% yield. Melting point: 196°C - 198°C. 1H NMR (500 MHz, DMSO- d_6) δ (ppm): 8.59 - 8.53 (m, 2H, CONH, benzene-H), 8.53 (s, 1H, pyrimidine-H), 8.48 (d, $J = 5.7$ Hz, 2H, pyridine-H), 8.38 (s, 1H, pyrimidine-NH-benzene), 7.29 (d, $J = 5.8$ Hz, 2H, pyridine-H), 7.09 (dd, $J = 10.8, 2.7$ Hz, 1H, benzene-H), 6.82 (td, $J = 8.7, 2.7$ Hz, 1H, benzene-H), 4.84 - 4.75 (m, 1H, $OCH(CH_3)_2$), 3.55 (q, $J = 6.8$ Hz, 2H, $CONHCH_2$), 2.89 (t, $J = 7.0$ Hz, 2H, CH_2 -pyridine), 2.78 (s, 3H, thiophene- CH_3), 1.32 (d, $J = 6.0$ Hz, 6H, $OCH(CH_3)_2$). ^{13}C NMR (126 MHz, DMSO- d_6) δ (ppm): 165.7, 162.5, 158.9 (d, $J_{C-F} = 240.3$ Hz), 156.1, 154.7, 149.9, 148.7, 148.6 (d, $J_{C-F} = 10.5$ Hz), 130.9, 128.9, 125.5 (d, $J_{C-F} = 2.5$ Hz), 124.8, 122.2 (d, $J = 9.5$ Hz), 117.5, 106.5 (d, $J_{C-F} = 21.8$ Hz), 101.5 (d, $J_{C-F} = 27.1$ Hz), 71.8, 34.4, 22.2, 16.2. HRMS calculated for $(M+H)^+$ 466.1708, found 466.1709. HPLC purity: 97.6%; retention time: 21.95 min.

4.9.24 4-((4-fluoro-2-methoxyphenyl)amino)-5-methylthieno[2,3-d]pyrimidin-6-yl)(4-methylpiperazin-1-yl)methanone (**7p**)

Compound **7p** was prepared from 1-methylpiperazine and **5a** using general procedure as a white solid in 32% yield. Melting point: 233°C - 235°C. 1H NMR (500 MHz, DMSO- d_6) δ (ppm): 8.46 (s, 1H, pyrimidine-H), 8.25 (s, 1H, pyrimidine-NH-benzene), 8.22 (dd, $J = 8.9, 6.4$ Hz, 1H, benzene-H), 7.07 (dd, $J = 10.7, 2.7$ Hz, 1H, benzene-H), 6.84 (td, $J = 8.7, 2.7$ Hz, 1H,

benzene-H), 3.88 (s, 3H, OCH₃), 3.68 - 3.39 (m, 4H, CON(CH₂)₂), 2.64 (s, 3H, thiophene-CH₃), 2.37 - 2.29 (m, 4H, CH₂NCH₂), 2.20 (s, 3H, NCH₃). ¹³C NMR (126 MHz, CDCl₃) δ (ppm): 167.0, 163.3, 158.9 (d, *J*_{C-F} = 243.0 Hz), 155.9, 154.2, 149.5 (d, *J*_{C-F} = 9.8 Hz), 127.7, 127.2, 124.2 (d, *J*_{C-F} = 3.2 Hz), 121.6 (d, *J*_{C-F} = 9.0 Hz), 116.7, 106.9 (d, *J*_{C-F} = 21.6 Hz), 98.8 (d, *J*_{C-F} = 27.3 Hz), 56.3, 46.0, 15.8. HRMS calculated for (M+H)⁺ 416.1551, found 416.1553. HPLC purity: 98.9%; retention time: 16.93 min.

4.9.25 (4-((4-fluoro-2-isopropoxyphenyl)amino)-5-methylthieno[2,3-d]pyrimidin-6-yl)(4-methylpiperazin-1-yl)methanone (**7q**)

Compound **7q** was prepared from 1-methylpiperazine and **5b** using general procedure as a white solid in 32% yield. Melting point: 167°C - 170°C. ¹H NMR (500 MHz, DMSO-*d*₆) δ (ppm): 8.59 (dd, *J* = 9.0, 6.4 Hz, 1H, benzene-H), 8.54 (s, 1H, pyrimidine-H), 8.33 (s, 1H, pyrimidine-NH-benzene), 7.09 (dd, *J* = 10.8, 2.7 Hz, 1H, benzene-H), 6.82 (td, *J* = 8.8, 2.7 Hz, 1H, benzene-H), 4.83 - 4.75 (m, 1H, OCH(CH₃)₂), 3.67 - 3.39 (m, 4H, CON(CH₂)₂), 2.68 (s, 3H, thiophene-CH₃), 2.37 - 2.30 (m, 4H, CH₂NCH₂), 2.21 (s, 3H, NCH₃), 1.32 (d, *J* = 6.0 Hz, 6H, OCH(CH₃)₂). ¹³C NMR (126 MHz, DMSO-*d*₆) δ (ppm): 166.4, 162.6, 158.8 (d, *J*_{C-F} = 240.0 Hz), 155.9, 154.2, 148.5 (d, *J*_{C-F} = 10.7 Hz), 128.0, 127.5, 125.6 (d, *J*_{C-F} = 2.8 Hz), 121.9 (d, *J*_{C-F} = 9.2 Hz), 116.7, 106.4 (d, *J*_{C-F} = 21.5 Hz), 101.5 (d, *J*_{C-F} = 26.9 Hz), 71.8, 45.9, 22.1, 16.1. HRMS calculated for (M+H)⁺ 444.1864, found 444.1864. HPLC purity: 95.4%; retention time: 20.63 min.

4.9.26 (4-((4-fluoro-2-methoxyphenyl)amino)-5-methylthieno[2,3-d]pyrimidin-6-yl)(pyrrolidin-1-yl)methanone (**7r**)

Compound **7r** was prepared from tetrahydro pyrrole and **5a** using general procedure as a white solid in 59% yield. Melting point: 209°C. ¹H NMR (500 MHz, DMSO-*d*₆) δ (ppm): 8.46 (s, 1H, pyrimidine-H), 8.26 (s, 1H, pyrimidine-NH-benzene), 8.22 (dd, *J* = 8.8, 6.4 Hz, 1H, benzene-H), 7.06 (dd, *J* = 10.7, 2.7 Hz, 1H, benzene-H), 6.84 (td, *J* = 8.7, 2.7 Hz, 1H, benzene-H), 3.88 (s, 3H, OCH₃), 3.50 (t, *J* = 5.5 Hz, 2H, CONCH₂), 3.34 (t, *J* = 5.5 Hz, 2H, CONCH₂), 2.67 (s, 3H, thiophene-CH₃), 1.94 - 1.81 (m, 4H, CH₂-(CH₂)₂-CH₂). ¹³C NMR (126 MHz, DMSO-*d*₆) δ (ppm): 166.3, 162.3, 159.6 (d, *J*_{C-F} = 240.7 Hz), 156.5, 154.3, 152.2 (d, *J*_{C-F} = 10.4 Hz), 128.9, 128.2, 124.6 (d, *J*_{C-F} = 3.1 Hz), 124.0 (d, *J*_{C-F} = 9.6 Hz), 116.6, 106.6 (d, *J*_{C-F} = 21.8 Hz), 100.3 (d, *J*_{C-F} = 27.1 Hz), 57.1, 48.6, 46.4, 26.0, 24.5, 16.1. HRMS calculated for (M+H)⁺ 387.1286, found 387.1286. HPLC purity: 98.9%; retention time: 24.29 min.

4.9.27 (4-((4-fluoro-2-isopropoxyphenyl)amino)-5-methylthieno[2,3-*d*]pyrimidin-6-yl)(pyrrolidin-1-yl)methanone (**7s**)

Compound **7s** was prepared from tetrahydro pyrrole and **5b** using general procedure as a white solid in 90% yield. Melting point: 209°C - 212°C. ¹H NMR (500 MHz, DMSO-*d*₆) δ (ppm): 8.60 (dd, *J* = 9.0, 6.5 Hz, 1H, benzene-H), 8.54 (s, 1H, pyrimidine-H), 8.35 (s, 1H, pyrimidine-NH-benzene), 7.09 (dd, *J* = 10.8, 2.7 Hz, 1H, benzene-H), 6.82 (td, *J* = 8.8, 2.7 Hz, 1H, benzene-H), 4.83 - 4.75 (m, 1H, OCH(CH₃)₂), 3.50 (t, *J* = 5.6 Hz, 2H, CONCH₂), 3.34 (t, *J* = 5.6 Hz, 2H, CONCH₂), 2.72 (s, 3H, thiophene-CH₃), 1.94 - 1.80 (m, 4H, CH₂-(CH₂)₂-CH₂), 1.32 (d, *J* = 6.0 Hz, 6H, OCH(CH₃)₂). ¹³C NMR (126 MHz, DMSO-*d*₆) δ (ppm): 166.2, 162.2, 158.8 (d, *J*_{C-F} = 240.1 Hz), 155.9, 154.2, 148.4 (d, *J*_{C-F} = 10.3 Hz), 129.0, 127.9, 125.6 (d, *J*_{C-F} = 2.8 Hz), 121.8 (d, *J*_{C-F} = 9.4 Hz), 116.7, 106.4 (d, *J*_{C-F} = 21.7 Hz), 101.5 (d, *J*_{C-F} = 27.1 Hz), 71.8, 48.6, 46.4, 26.0, 24.4, 22.1, 16.1. HRMS calculated for (M+H)⁺ 415.1599, found 415.1597. HPLC purity: 97.9%; retention time: 25.17 min.

4.9.28 *N*-cyclohexyl-4-((4-fluoro-2-methoxyphenyl)amino)-5-methylthieno[2,3-*d*]pyrimidine-6-carboxamide (**7t**)

Compound **7t** was prepared from cyclohexylamine and **5a** using general procedure as a white solid in 42% yield. Melting point: 224°C - 226°C. ¹H NMR (500 MHz, DMSO-*d*₆) δ (ppm): 8.46 (s, 1H, pyrimidine-H), 8.35 - 8.28 (m, 2H, pyrimidine-NH-benzene, CONH), 8.20 (dd, *J* = 8.8, 6.4 Hz, 1H, benzene-H), 7.07 (dd, *J* = 10.7, 2.7 Hz, 1H, benzene-H), 6.84 (td, *J* = 8.7, 2.7 Hz, 1H, benzene-H), 3.88 (s, 3H, OCH₃), 3.78 - 3.71 (m, 1H, CONHCH), 2.82 (s, 3H, thiophene-CH₃), 1.89 - 1.80 (m, 2H, cyclohexane-H), 1.77 - 1.68 (m, 2H, cyclohexane-H), 1.62 - 1.59 (m, 1H, cyclohexane-H), 1.36-1.26 (m, 4H, cyclohexane-H), 1.18-1.08 (m, 1H, cyclohexane-H). ¹³C NMR (126 MHz, DMSO-*d*₆) δ (ppm): 165.8, 161.7, 159.7 (d, *J*_{C-F} = 240.7 Hz), 156.7, 154.6, 152.3 (d, *J*_{C-F} = 10.5 Hz), 130.3, 129.5, 124.5 (d, *J*_{C-F} = 3.1 Hz), 124.3 (d, *J*_{C-F} = 9.4 Hz), 117.3, 106.6 (d, *J*_{C-F} = 21.9 Hz), 100.3 (d, *J*_{C-F} = 27.1 Hz), 57.1, 49.2, 32.7, 25.6, 25.2, 16.3. HRMS calculated for (M+H)⁺ 415.1599, found 415.1600. HPLC purity: 97.9%; retention time: 27.67 min.

4.9.29 *N*-cyclohexyl-4-((4-fluoro-2-isopropoxyphenyl)amino)-5-methylthieno[2,3-*d*]pyrimidine-6-carboxamide (**7u**)

Compound **7u** was prepared from cyclohexylamine and **5b** using general procedure as a white solid in 69% yield. Melting point: 227°C - 230°C. ¹H NMR (500 MHz, DMSO-*d*₆) δ (ppm): 8.56 (dd, *J* = 9.0, 6.5 Hz, 1H, benzene-H), 8.53 (s, 1H, pyrimidine-H), 8.38 (s, 1H, pyrimidine-NH-benzene), 8.34 (d, *J* = 7.8 Hz, 1H, CONH), 7.10 (dd, *J* = 10.8, 2.7 Hz, 1H, benzene-H), 6.82 (td, *J* = 8.7, 2.7 Hz, 1H, benzene-H), 4.84 - 4.76 (m, 1H, OCH(CH₃)₂), 3.78 - 3.69 (m, 1H, CONHCH), 2.87 (s, 3H, thiophene-CH₃), 1.89 - 1.79 (m, 2H, cyclohexane-H), 1.77 - 1.68 (m,

2H, cyclohexane-H), 1.62 - 1.56 (m, 1H, cyclohexane-H), 1.37 - 1.25 (m, 10H, cyclohexane-H, OCH(CH₃)₂), 1.18-1.08 (m, 1H, cyclohexane-H). ¹³C NMR (126 MHz, DMSO-*d*₆) δ (ppm): 165.7, 161.6, 158.9 (d, *J*_{C-F} = 240.1 Hz), 156.1, 154.6, 148.7 (d, *J*_{C-F} = 10.4 Hz), 130.1, 129.6, 125.5 (d, *J*_{C-F} = 2.9 Hz), 122.3 (d, *J*_{C-F} = 9.3 Hz), 117.4, 106.5 (d, *J*_{C-F} = 21.8 Hz), 101.5 (d, *J*_{C-F} = 27.0 Hz), 71.8, 49.2, 32.7, 25.6, 25.2, 22.2, 16.3. HRMS calculated for (M+H)⁺ 443.1912, found 443.1910. HPLC purity: 96.5%; retention time: 30.02 min.

4.9.30 *N*-(3-(dimethylamino)propyl)-4-((4-fluoro-2-methoxyphenyl)amino)-5-methylthieno[2,3-*d*]pyrimidine-6-carboxamide (7v)

White powder (56.4%); melting point: 139°C - 141°C; ¹H NMR (500 MHz, DMSO-*d*₆) δ 8.54 (t, *J* = 5.5 Hz, 1H, CONH), 8.46 (s, 1H, pyrimidine-H), 8.32 (s, 1H, pyrimidine-NH-benzene), 8.19 (dd, *J* = 8.9, 6.2 Hz, 1H, benzene-H), 7.06 (dd, *J* = 10.7, 2.7 Hz, 1H, benzene-H), 6.84 (td, *J* = 8.7, 2.7 Hz, 1H, benzene-H), 3.88 (s, 3H, OCH₃), 3.28 (q, *J* = 6.7 Hz, 2H, CONHCH₂), 2.87 (s, 3H, thiophene-CH₃), 2.28 (t, *J* = 6.9 Hz, 2H, CH₂N), 2.15 (s, 6H, N(CH₃)₂), 1.70 - 1.63 (m, 2H, CH₂CH₂CH₂); ¹³C NMR (126 MHz, DMSO-*d*₆) δ 165.8, 162.4, 159.8 (d, *J*_{C-F} = 240.9 Hz), 156.8, 154.7, 152.4 (d, *J*_{C-F} = 10.5 Hz), 131.2, 128.9, 124.5 (d, *J* = 3.1 Hz), 124.4 (d, *J* = 9.4 Hz), 117.5, 106.6 (d, *J*_{C-F} = 21.9 Hz), 100.3 (d, *J*_{C-F} = 27.1 Hz), 57.5, 57.1, 45.6, 38.7, 27.1, 16.2; HRMS calcd for (M + H)⁺ 418.1708, found 418.1711.

4.9.31 *N*-(3-(dimethylamino)propyl)-4-((4-fluoro-2-isopropoxyphenyl)amino)-5-methylthieno[2,3-*d*]pyrimidine-6-carboxamide (7w)

White powder (34.3%); melting point: 169°C - 171°C; ¹H NMR (500 MHz, DMSO-*d*₆) δ 8.60 - 8.54 (m, 2H, CONH, benzene-H), 8.53 (s, 1H, pyrimidine-H), 8.41 (s, 1H, pyrimidine-NH-benzene), 7.10 (dd, *J* = 10.8, 2.6 Hz, 1H, benzene-H), 6.82 (td, *J* = 8.7, 2.6 Hz, 1H, benzene-H),

4.84 - 4.75 (m, 1H, OCH(CH₃)₂), 3.28 (q, $J = 5.2$ Hz, 2H, CONHCH₂), 2.91 (s, 3H, thiophene-CH₃), 2.28 (t, $J = 6.9$ Hz, 2H, CH₂N), 2.14 (s, 6H, N(CH₃)₂), 1.70 - 1.63 (m, 2H, CH₂CH₂CH₂), 1.32 (d, $J = 6.0$ Hz, 6H, OCH(CH₃)₂). ¹³C NMR (126 MHz, DMSO-*d*₆) δ 165.7, 162.4, 158.8 (d, $J_{C-F} = 240.2$ Hz), 156.1, 154.7, 148.6 (d, $J_{C-F} = 10.3$ Hz), 130.9, 129.1, 125.5 (d, $J_{C-F} = 2.9$ Hz), 122.2 (d, $J_{C-F} = 9.4$ Hz), 117.6, 106.5 (d, $J_{C-F} = 21.7$ Hz), 101.5 (d, $J_{C-F} = 26.9$ Hz), 71.8, 57.5, 45.6, 38.7, 27.1, 22.1, 16.2; HRMS calcd for (M + H)⁺ 446.2021, found 446.2022.

4.8.32 4-((4-fluoro-2-isopropoxyphenyl)amino)-*N*-(3-hydroxypropyl)-5-methylthieno[2,3-*d*]pyrimidine-6-carboxamide (**7x**)

White powder (74.6%); melting point: 167°C - 170°C; ¹H NMR (500 MHz, DMSO-*d*₆) δ 8.57 (dd, $J = 9.0, 6.4$ Hz, 1H, benzene-H), 8.53 (s, 1H, pyrimidine-H), 8.43 (t, $J = 5.5$ Hz, 1H, CONH), 8.40 (s, 1H, pyrimidine-NH-benzene), 7.09 (dd, $J = 10.8, 2.7$ Hz, 1H, benzene-H), 6.82 (td, $J = 8.7, 2.8$ Hz, 1H, benzene-H), 4.83 - 4.76 (m, 1H, OCH(CH₃)₂), 4.51 (t, $J = 5.2$ Hz, 1H, OH), 3.48 (q, $J = 6.2$ Hz, 2H, CH₂CH₂CH₂OH), 2.90 (s, 3H, thiophene-CH₃), 1.73 - 1.65 (m, 2H, CH₂CH₂CH₂OH), 1.32 (d, $J = 6.0$ Hz, 6H, OCH(CH₃)₂). (two hydrogens signal overlap with water peak) ¹³C NMR (126 MHz, DMSO-*d*₆) δ 165.7, 162.5, 158.9 (d, $J_{C-F} = 239.8$ Hz), 156.1, 154.7, 148.6 (d, $J_{C-F} = 10.3$ Hz), 130.8, 129.1, 125.5 (d, $J_{C-F} = 2.9$ Hz), 122.3 (d, $J_{C-F} = 9.6$ Hz), 117.6, 106.5 (d, $J_{C-F} = 21.9$ Hz), 101.5 (d, $J_{C-F} = 26.9$ Hz), 71.8, 59.1, 37.4, 32.7, 22.1, 16.3; HRMS calcd for (M + H)⁺ 419.1548, found 419.1548.

ASSOCIATED CONTENT

Supplementary Material

Additional figures and tables, NMR spectra and other data related to characterization of all compounds presented in current manuscript are included in the supplementary material.

AUTHOR INFORMATION

Corresponding Author

***E-mail:** Tao Jiang. (email: jiangtao@ouc.edu.cn; Tel: +86 532 82033054) or Christopher G. Proud (email: Christopher.Proud@sahmri.com; Tel: +61 8 8128 4810)

Author Contributions

The manuscript was written through contributions of all authors. All authors have approved the final version of the manuscript.

#Xin Jin, James Merrett contributed equally and should be considered as joint first authors.

Notes

The authors declare no competing financial interest.

ACKNOWLEDGEMENTS

The authors are grateful for financial support granted by NSFC-Shandong Joint Fund (U1706213, U1406403), Innovation Project from Qingdao National Laboratory for Marine Science and Technology (No.2015ASKJ02), the Fundamental Research Funds for the Central Universities

(No. 201512007, 201762011 for R.Y.). We also acknowledge financial support from the South Australian Health and Medical Research Institute. The 3T3-L1 pre-adipocytes were a kind gift from Associate Professor Yeesim Khew-Goodall from the Centre for Cancer Biology (SA Pathology), Adelaide, Australia.

ABBREVIATIONS USED

MNK, mitogen activated protein kinase interacting kinase; eIF4E, eukaryotic translation initiation factor4E; mTORC1, mammalian target of rapamycin complex 1; TLC, thin layer chromatography; EDCI, 1-ethyl-3-(3-dimethylaminopropyl)carbodiimide.

REFERENCES

- [1] R. Fukunaga, T. Hunter, MNK1, a new MAP kinase-activated protein kinase, isolated by a novel expression screening method for identifying protein kinase substrates, *EMBO J*, 16 (1997) 1921-1933.
- [2] X. Wang, A. Flynn, A.J. Waskiewicz, B.L. Webb, R.G. Vries, I.A. Baines, J.A. Cooper, C.G. Proud, The phosphorylation of eukaryotic initiation factor eIF4E in response to phorbol esters, cell stresses, and cytokines is mediated by distinct MAP kinase pathways, *J Biol Chem*, 273 (1998) 9373-9377.
- [3] A.J. Waskiewicz, A. Flynn, C.G. Proud, J.A. Cooper, Mitogen-activated protein kinases activate the serine/threonine kinases Mnk1 and Mnk2, *EMBO J*, 16 (1997) 1909-1920.
- [4] A.J. Waskiewicz, J.C. Johnson, B. Penn, M. Mahalingam, S.R. Kimball, J.A. Cooper, Phosphorylation of the cap-binding protein eukaryotic translation initiation factor 4E by protein kinase Mnk1 in vivo, *Mol Cell Biol*, 19 (1999) 1871-1880.
- [5] G.C. Scheper, N.A. Morrice, M. Kleijn, C.G. Proud, The mitogen-activated protein kinase signal-integrating kinase Mnk2 is a eukaryotic initiation factor 4E kinase with high levels of basal activity in mammalian cells, *Mol Cell Biol*, 21 (2001) 743-754.
- [6] A.C. Gingras, B. Raught, N. Sonenberg, eIF4 initiation factors: effectors of mRNA recruitment to ribosomes and regulators of translation, *Annu Rev Biochem*, 68 (1999) 913-963.
- [7] C.G. Proud, Mnks, eIF4E phosphorylation and cancer, *Biochim Biophys Acta*, 1849 (2015) 766-773.
- [8] E. Lineham, J. Spencer, S.J. Morley, Dual abrogation of MNK and mTOR: a novel therapeutic approach for the treatment of aggressive cancers, *Future Med Chem*, 9 (2017) 1539-1555.

- [9] L. Furic, L. Rong, O. Larsson, I.H. Koumakpayi, K. Yoshida, A. Brueschke, E. Petroulakis, N. Robichaud, M. Pollak, L.A. Gaboury, P.P. Pandolfi, F. Saad, N. Sonenberg, eIF4E phosphorylation promotes tumorigenesis and is associated with prostate cancer progression, *Proc Natl Acad Sci U S A*, 107 (2010) 14134-14139.
- [10] T. Ueda, M. Sasaki, A.J. Elia, Chio, II, K. Hamada, R. Fukunaga, T.W. Mak, Combined deficiency for MAP kinase-interacting kinase 1 and 2 (Mnk1 and Mnk2) delays tumor development, *Proc Natl Acad Sci U S A*, 107 (2010) 13984-13990.
- [11] T. Teo, M. Yu, Y. Yang, T. Gillam, F. Lam, M.J. Sykes, S. Wang, Pharmacologic co-inhibition of Mnks and mTORC1 synergistically suppresses proliferation and perturbs cell cycle progression in blast crisis-chronic myeloid leukemia cells, *Cancer Lett*, 357 (2015) 612-623.
- [12] J.E. Beggs, S. Tian, G.G. Jones, J. Xie, V. Iadevaia, V. Jenei, G. Thomas, C.G. Proud, The MAP kinase-interacting kinases regulate cell migration, vimentin expression and eIF4E/CYFIP1 binding, *Biochem J*, 467 (2015) 63-76.
- [13] Y. Zhan, J. Guo, W. Yang, C. Goncalves, T. Rzymiski, A. Dreas, E. Zylkiewicz, M. Mikulski, K. Brzozka, A. Golas, Y. Kong, M. Ma, F. Huang, B. Huor, Q. Guo, S.D. da Silva, J. Torres, Y. Cai, I. Topisirovic, J. Su, K. Bijian, M.A. Alaoui-Jamali, S. Huang, F. Journe, G.E. Ghanem, W.H. Miller, Jr., S.V. Del Rincon, MNK1/2 inhibition limits oncogenicity and metastasis of KIT-mutant melanoma, *J Clin Invest*, 127 (2017) 4179-4192.
- [14] N. Robichaud, S.V. del Rincon, B. Huor, T. Alain, L.A. Petruccielli, J. Hearnden, C. Goncalves, S. Grotegut, C.H. Spruck, L. Furic, O. Larsson, W.J. Muller, W.H. Miller, N. Sonenberg, Phosphorylation of eIF4E promotes EMT and metastasis via translational control of SNAIL and MMP-3, *Oncogene*, 34 (2015) 2032-2042.
- [15] B. Herdy, M. Jaramillo, Y.V. Svitkin, A.B. Rosenfeld, M. Kobayashi, D. Walsh, T. Alain, P. Sean, N. Robichaud, I. Topisirovic, L. Furic, R.J.O. Dowling, A. Sylvestre, L. Rong, R. Colina, M. Costa-Mattioli, J.H. Fritz, M. Olivier, E. Brown, I. Mohr, N. Sonenberg, Translational control of the activation of transcription factor NF-kappaB and production of type I interferon by phosphorylation of the translation factor eIF4E, *Nat Immunol*, 13 (2012) 543-550.
- [16] X. Su, Y. Yu, Y. Zhong, E.G. Giannopoulou, X. Hu, H. Liu, J.R. Cross, G. Ratsch, C.M. Rice, L.B. Ivashkiv, Interferon-gamma regulates cellular metabolism and mRNA translation to potentiate macrophage activation, *Nat Immunol*, 16 (2015) 838-849.
- [17] C.E. Moore, J. Pickford, F.R. Cagampang, R.L. Stead, S. Tian, X. Zhao, X. Tang, C.D. Byrne, C.G. Proud, MNK1 and MNK2 mediate adverse effects of high-fat feeding in distinct ways, *Sci Rep*, 6 (2016) 23476.
- [18] T. Ueda, R. Watanabe-Fukunaga, H. Fukuyama, S. Nagata, R. Fukunaga, Mnk2 and Mnk1 are essential for constitutive and inducible phosphorylation of eukaryotic initiation factor 4E but not for cell growth or development, *Mol Cell Biol*, 24 (2004) 6539-6549.
- [19] C. Tschopp, U. Knauf, M. Brauchle, M. Zurini, P. Ramage, D. Glueck, L. New, J. Han, H. Gram, Phosphorylation of eIF-4E on Ser 209 in response to mitogenic and inflammatory stimuli is faithfully detected by specific antibodies, *Mol Cell Biol Res Commun*, 3 (2000) 205-211.
- [20] J. Bain, L. Plater, M. Elliott, N. Shpiro, C.J. Hastie, H. McLauchlan, I. Klevernic, J.S. Arthur, D.R. Alessi, P. Cohen, The selectivity of protein kinase inhibitors: a further update, *Biochem J*, 408 (2007) 297-315.
- [21] S. Santag, F. Siegel, A.M. Wengner, C. Lange, U. Bomer, K. Eis, F. Puhler, P. Lienau, L. Bergemann, M. Michels, F. von Nussbaum, D. Mumberg, K. Petersen, BAY 1143269, a novel MNK1 inhibitor, targets oncogenic protein expression and shows potent anti-tumor activity, *Cancer Lett*, 390 (2017) 21-29.

- [22] A. Dreas, M. Mikulski, M. Milik, C.H. Fabritius, K. Brzozka, T. Rzymiski, Mitogen-activated Protein Kinase (MAPK) Interacting Kinases 1 and 2 (MNK1 and MNK2) as Targets for Cancer Therapy: Recent Progress in the Development of MNK Inhibitors, *Curr Med Chem*, 24 (2017) 3025-3053.
- [23] E.M. Kosciuczuk, D. Saleiro, B. Kroczyńska, E.M. Beauchamp, F. Eckerdt, G.T. Blyth, S.M. Abedin, F.J. Giles, J.K. Altman, L.C. Plataniias, Merestinib blocks Mnk kinase activity in acute myeloid leukemia progenitors and exhibits antileukemic effects in vitro and in vivo, *Blood*, 128 (2016) 410-414.
- [24] H. Yang, L.R. Chennamaneni, M.W.T. Ho, S.H. Ang, E.S.W. Tan, D.A. Jeyaraj, Y.S. Yeap, B. Liu, E.H. Ong, J.K. Joy, J.L.K. Wee, P. Kwek, P. Retna, N. Dinie, T.T.H. Nguyen, S.J. Tai, V. Manoharan, V. Pendharkar, C.B. Low, Y.S. Chew, S. Vuddagiri, K. Sangthongpitag, M.L. Choong, M.A. Lee, S. Kannan, C.S. Verma, A. Poulsen, S. Lim, C. Chuah, T.S. Ong, J. Hill, A. Matter, K. Nacro, Optimization of Selective Mitogen-Activated Protein Kinase Interacting Kinases 1 and 2 Inhibitors for the Treatment of Blast Crisis Leukemia, *J Med Chem*, 61 (2018) 4348-4369.
- [25] T. Teo, Y. Yang, M. Yu, S.K. Basnet, T. Gillam, J. Hou, R.M. Schmid, M. Kumarasiri, S. Diab, H. Albrecht, M.J. Sykes, S. Wang, An integrated approach for discovery of highly potent and selective Mnk inhibitors: Screening, synthesis and SAR analysis, *Eur J Med Chem*, 103 (2015) 539-550.
- [26] M. Yu, P. Li, S.K. Basnet, M. Kumarasiri, S. Diab, T. Teo, H. Albrecht, S. Wang, Discovery of 4-(dihydropyridinon-3-yl)amino-5-methylthieno[2,3-d]pyrimidine derivatives as potent Mnk inhibitors: synthesis, structure-activity relationship analysis and biological evaluation, *Eur J Med Chem*, 95 (2015) 116-126.
- [27] S. Diab, P. Li, S.K. Basnet, J. Lu, M. Yu, H. Albrecht, R.W. Milne, S. Wang, Unveiling new chemical scaffolds as Mnk inhibitors, *Future Med Chem*, 8 (2016) 271-285.
- [28] S. Diab, A.M. Abdelaziz, P. Li, T. Teo, S.K.C. Basnet, B. Noll, M.H. Rahaman, J. Lu, J. Hou, M. Yu, B.T. Le, H. Albrecht, R.W. Milne, S. Wang, Dual Inhibition of Mnk2 and FLT3 for potential treatment of acute myeloid leukaemia, *Eur J Med Chem*, 139 (2017) 762-772.
- [29] M. Buxade, J.L. Parra-Palau, C.G. Proud, The Mnks: MAP kinase-interacting kinases (MAP kinase signal-integrating kinases), *Front Biosci*, 13 (2008) 5359-5373.
- [30] S. Vilar, G. Cozza, S. Moro, Medicinal chemistry and the molecular operating environment (MOE): application of QSAR and molecular docking to drug discovery, *Curr Top Med Chem*, 8 (2008) 1555-1572.
- [31] R. Jauch, S. Jakel, C. Netter, K. Schreiter, B. Aicher, H. Jackle, M.C. Wahl, Crystal structures of the Mnk2 kinase domain reveal an inhibitory conformation and a zinc binding site, *Structure*, 13 (2005) 1559-1568.
- [32] J. Oyarzabal, N. Zarich, M.I. Albarran, I. Palacios, M. Urbano-Cuadrado, G. Mateos, I. Reymundo, O. Rabal, A. Salgado, A. Corrienero, J. Fominaya, J. Pastor, J.R. Bischoff, Discovery of mitogen-activated protein kinase-interacting kinase 1 inhibitors by a comprehensive fragment-oriented virtual screening approach, *J Med Chem*, 53 (2010) 6618-6628.
- [33] W. Han, Y. Ding, Y. Xu, K. Pfister, S. Zhu, B. Warne, M. Doyle, M. Aikawa, P. Amiri, B. Appleton, D.D. Stuart, A. Fanidi, C.M. Shafer, Discovery of a Selective and Potent Inhibitor of Mitogen-Activated Protein Kinase-Interacting Kinases 1 and 2 (MNK1/2) Utilizing Structure-Based Drug Design, *J Med Chem*, 59 (2016) 3034-3045.

- [34] A. Flynn, C.G. Proud, Serine 209, not serine 53, is the major site of phosphorylation in initiation factor eIF-4E in serum-treated Chinese hamster ovary cells, *J Biol Chem*, 270 (1995) 21684-21688.
- [35] M.C. Brown, M. Gromeier, MNK Controls mTORC1:Substrate Association through Regulation of TELO2 Binding with mTORC1, *Cell Rep*, 18 (2017) 1444-1457.
- [36] S. Tian, X. Wang, C.G. Proud, Oncogenic MNK signalling regulates the metastasis suppressor NDRG1, *Oncotarget*, 8 (2017) 46121-46135.
- [37] A.D. Barlow, J. Xie, C.E. Moore, S.C. Campbell, J.A. Shaw, M.L. Nicholson, T.P. Herbert, Rapamycin toxicity in MIN6 cells and rat and human islets is mediated by the inhibition of mTOR complex 2 (mTORC2), *Diabetologia*, 55 (2012) 1355-1365.

Highlights

1. The MNK protein kinases (MNK1/2) play roles in cancer and metabolic disease
2. From a set of 28 thienopyrimidines, 15 MNK inhibitors were identified
3. One compound in particular, termed **7g**, shows selectivity for MNK2 compared to MNK1
4. Molecular docking revealed two H-bonds that are important for binding to MNKs